Department of Electrical and Computer Systems Engineering

Technical Report
MECSE-4-2005

DWDM Optically Amplified Transmission Systems - SIMULINK Models and Test-Bed: Part III ‑DPSK

L.N. Binh and Y.L.Cheung

MONASH
UNIVERSITY

DWDM OPTICALLY AMPLIFIED TRANSMISSION SYSTEMS -
SIMULINK MODELS AND TEST-BED: PART III –DPSK
MODULATION FORMAT

L.N. Binh and D. Wong

*Department of Electrical and Computer Systems Engineering, Monash University,
Clayton, Victoria 3168 Australia email; le.nguyen.binh@eng.monash.edu.au*

Abstract

A simulator based on Matlab™ Simulink for simulation of optical communication systems employing DPSK modulation format and RZ and NRZ pulse profile is described. The simulator for optically amplified transmission systems (SOATS) is described in details with simulink blocks and monitored with several scopes.

The choice modulation format used is very important to minimize the fiber dispersion and impairments due to nonlinear effects. Dispersion can be compensated with the use of dispersion compensating fibers. Experimental set-up and results are included and compared with simulated system performance. Simulink blocks of the simulator system design are described, conferred and proven with experimental results. Various modulation formats developed for the Simulink simulator are also described. Experimental results are confirmed with analytically simulated results. Phase modulation formats have been considered and implemented using MATLAB SIMULINK. The NRZ, RZ, NRZ-DPSK and RZ-DPSK transmission and demodulation are designed and demonstrated. This MatLab Simulink model allows simulation of novel advanced optical communications systems.

1

CONTENTS

TABLE OF FIGURES

4

5

6

1. INTRODUCTION

As photonic technology advances, there has been tremendous development in transmission systems especially in optical communication systems. With the increase traffic in data transmission, engineers now aim to transmit over longer distance and at a faster rate with less dispersion.

This work presents the MATLAB SIMULINK model of a Dense Wavelength Division Multiplexed (DWDM) 10 Gb/s Communications Systems incorporating several modulation formats. To the best of our knowledge, this MATLAB SIMULINK simulator has been implemented for the first time, for optically amplified transmission systems (SOATS).

The simulator enables transmission of several optical channels through spans of single mode fiber and dispersion compensating fibres and different modulation formats, especially the differential phase shift-keying (DPSK) technique in this part I. DWDM technology requires photonic devices including optical transmitters, multiplers and demultiplexers and receivers[1], optical amplifiers and fibers. The spacing between channels in the frequency domain determines the complexity of these photonic devices and the power penalty and hence the budget of the transmission systems. The use of an optical amplifier, the EDFAs, enables us to compensate for losses and attenuation through various components and propagation through the guide media (the transmission and dispersion compensating fibers). With the use of the EDFA, the signals or PRBS pattern can be amplified simultaneously.

To improve system transmission performance for the 10 Gb/s and/or 40 Gb/s DWDM system, advanced modulation formats are attracting considerable interests. Modulation

7

formats that have a narrow spectral width and concentration of optical energy over the signal bands and low susceptibility to fiber non-linearity, error-free transmission performance and with large dispersion tolerance are considered in this paper.

The paper is organized as follows: Section 2 outlines the basic properties of photonic components of an optical fiber communication system and fundamental properties for Simulink representation, Section 3 describes experimental equipment set-up of the test bed demonstration for the 10 Gb/s NRZ–ASK and 40 Gb/s DPSK schemes. Section 4 then describes the experimental results obtained for NRZ ASK and details of the Simulink models. Further simulated results for NRZ ASK for back to back and transmission over 0 Km SSMF are presented. Other modulation formats, especially the DPSK are given with back-to-back measurements of the BER as a function of receiver sensitivity. Finally Section 5 outlines the challenges and gives a summary of the simulator.

2. TRANSMISSION SYSTEMS AND PHOTONIC COMPONENTS

2.1. Transmission Systems

A general optical communication system usually consists of multiplexes, fibers, receivers, and modulators. Figure 1 shows a general optical communication system [2].
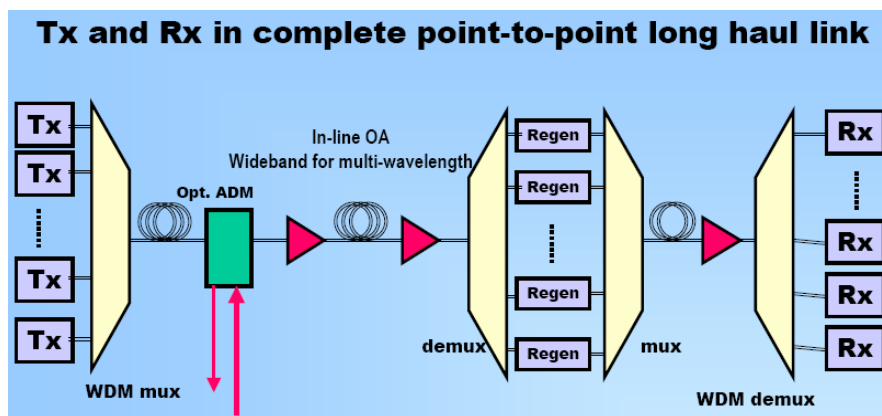
Figure 1: General optically amplified communication system diagram

To design the transmitter section of the optical communication system, it is essential to know how to modulate an optical signal from the electrical domain. Optical transmitters generate signals that carry the carrier by modulating the intensity of an optical carrier

8

generated by a light source, the DFB laser. The modulation can then be performed using an electro-optic or electro-absorption modulator to change the intensity of the lightwaves emitting from the light source. To minimize transmission impairments du e to dispersion and nonlinear effects, the modulation format chosen to transmit signals in the fiber optic communications system is very important.

A transmitter generates a signal in a form for transmission, while a receiver detects the signal and converts it to a usable form. WDM is the optical technology that couples many wavelength carrier lightwaves transmitting over the same single mode fiber. This increases the aggregate bandwidth per single fiber to integrate the bit-rate of all wavelength channels. DWDM technology offers larger (denser) number of wavelengths coupled into a fiber compared to WDM with closer spacing between carries of the channels.

2.2. *The Mach-Zehnder Interferometer Modulator*

Lightwaves must be modulated to transmit a signal; and for high performance systems, external modulation is usually used. The Mach-Zehnder Interferometer Modulator (MZIM) is described here due to superior and flexibility in use as compared with the EA modulator or direct modulation technique. This is due to the change in the refractive index of some materials when an electric field, usually via a bias and a traveling RF wave iapplied to the electrodes. This affects the material almost instantly the lightwves passing through the modulator. Hence the electro-optic refractive index change is proportional to the voltage applied to the material. Delaying the light phase causes interference effects that modulate the output intensity constructively or destructively as illustrated in Figure 2 [2].

(a)   (b)
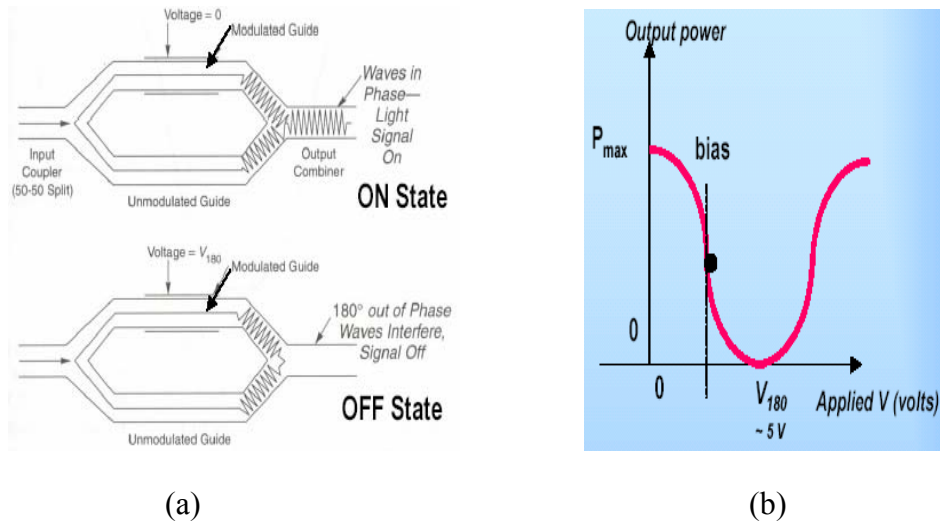
Figure 2: Mach-Zehnder (a) configuration and operation.[2] (b) The V-P transfer characteristics of the Mach-Zehnder modulator.

2.3.   Modulation

The ideal modulation formats for long haul and high speed DWDM transmission system are dispersion tolerant and resilient to nonlinear effects. The modulation formats that are considered in this DWDM 10Gb/s communications systems can be based on the phase modulation of the carriers under the signal envelops and amplitude modulation. They can be classified as:

Amplitude Modulation Formats

- Return –to-zero On/Off Keying (RZ-OOK or RZ-ASK)

- Carrier-Suppressed Return-to-Zero (CSRZ-OOK or CSRZ-ASK) and

- Non-Return-to Zero On/Off Keying (NRZ-OOK)

Phase Modulation Formats

- Non-return-to-zero Differential Phase Keying (NRZ-DPSK) and NRZ-DQPSK

- Return-to Zero Differential Phase Keying(RZ-DPSK) and

- RZ-DQPSK or CSRZ-DPSK and CS-DQPSK

10

Experimentally, in the first stage the modulation format used in the experiment is the NRZ-OOK format and demonstrated hrewith. Hence the SIMULINK model design of the system is also designed using the NRZ-OOK modulation format. Other modulation formats have also been implemented.

2.4. Optical Fibers

Optical fibers are the transporting medium for optical communication systems. A typical optical fiber is made of ultra pure silica doped with impurities to increase the refractive index of the fiber. One of the major problems experienced in optical communication systems is dispersion. The types of dispersion faced are mainly, chromatic dispersion and polarization mode dispersion (PMD). Hence we could represent the dispersion as Fiber Dispersion = Chromatic + PMD + Dispersion due to non-linear effects.

Chromatic dispersion is a property of optical fibers that can limit the performance of an optical fiber communications system. Chromatic dispersion is the sum of two quantities; dispersion inherent to the material and dispersion that arise from the structure of the waveguide.

$$D_T = D_M + D_{wg} \tag{1}$$

where D_T = Total Chromatic Dispersion, D_M = Material Dispersion, D_{wg} = Waveguide Dispersion.

The propagation characteristic of each wavelength depends on the refractive index of the medium. As wavelength travel at different speeds in the fiber; material dispersion occurs. Therefore when light is passed through the fiber, each individual wavelength arrives at the end of the fiber at different times; therefore causing pulse broadening. Waveguide dispersion is due to the lightwave group traveling velocity as function of fiber geometrical parameters and index profile. Hence Waveguide dispersion arises from the distribution of light between the fiber core and cladding.

Chromatic dispersion is the effect of pulse spreading or broadening and can reduce the integrity of a received signal unless appropriate dispersion modules are included in the optical communication system. Further lightwaves transmission in a single mode fiber

11

(SMF) is affected by a property of light known as polarization. The fields are perpendicular to each other and to the direction that light travels. Normal light is considered a combination of two polarizations, vertical and horizontal which is determined by the direction of the electric field. Polarization is important in SMF as SMF actually carries two modes with orthogonal polarization. Hence the fiber with circular symmetry cores cannot differentiate between the two polarizations causing the light to shift easily between the two polarization modes. As light travels along the fiber at different speeds, the two polarization modes will experience slightly different conditions. This effect is known as the polarization mode dispersion (PMD).

2.5. *Optical Receivers*

Receivers are the final sector in any communication system. The optical receivers convert an optical signal to electrical RF signals and re-sampled to the digital forms. The design of an optical receiver depends on the modulation format of the signals. In a WDM communications system, the muxed signals must be demuxed into its composite wavelengths so that each optical channel can be directed to separate receivers[3]. This separation is very important as the photodetectors are usually color-blind, very broad spectrum to wavelength. Electrons are then amplified and processed back to digital domain.
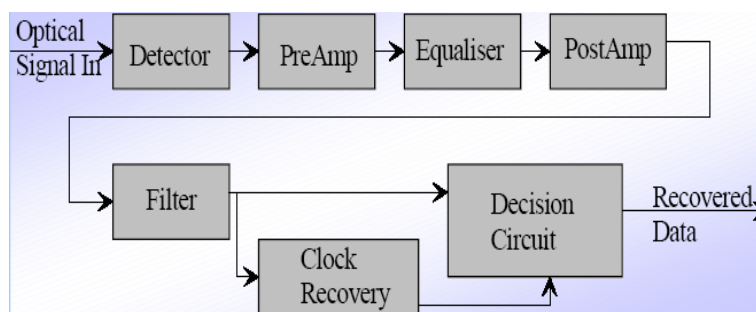
Figure 3: Block diagram of an optical digital receiver[2]

3. EXPERIMENTAL SETUP AND RESULTS

A series of experiment was conducted. This section outlines the equipment set-up and details of the equipment.

3.1. Equipment and Photonic Hardware

Figure 4 shows an optical spectrum analyzer. This instrument was used to analyze the optical signal in frequency domain, in terms of signal strength (dB) and wavelength.

Figure 4*: Optical Spectrum Analyzer*

The series spectrum analyzer as seen in Figure 5 was used to analyze the electrical signal in the frequency domain. This device operates in a lower frequency than the optical spectrum analyzer. When coupled with a photo detector, the modulating signal which is the envelope of the optical signal can be observed.
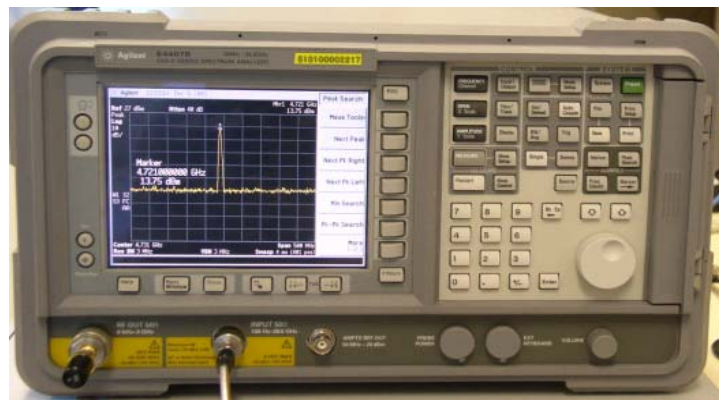
Figure 5*: Series Spectrum Analyzer*

Figure 6 shows a power supply that was used to provide a D.C voltage when finding the Vbias of the MZIM.

13

Figure 6*: Power Supply*

The Pulse Pattern Generator in Figure 7 is capable of generating different bit patterns for testing purposes. The output was connected into the input of the MZIM.

Figure 7*: Pulse Pattern Generator*

This device as seen in Figure 8 operates similarly to a normal signal generator except for its high frequency capability.

Figure 8*: Synthesized Signal Generator (10MHz to 20GHz)*

Figure 9*: Current-Limited Power Supply*

The Current-Limited power supply in Figure 9 was used to supply positive and negative voltage to the photo detector.
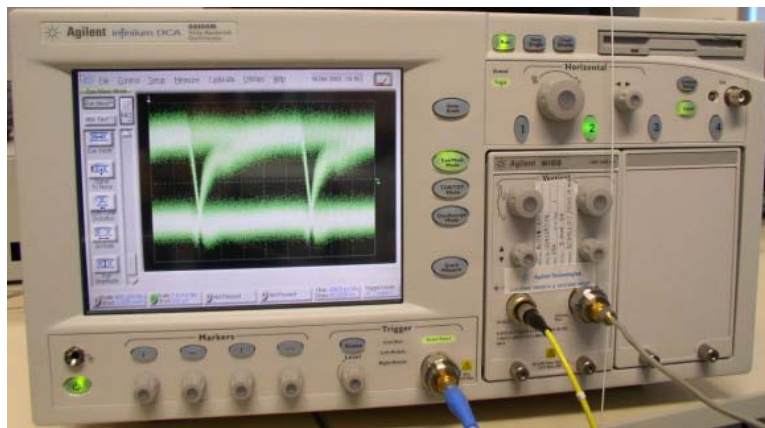
Figure 10: Digital Communications Analyzer

The 86100C Digital Communications Analyzer with jitter analysis (DCA-J) in Figure 10 offers four instruments in one. A digital communications analyzer with automated eye measurements; a full-function time domain reflect meter (TDR) for impedance analysis; a full-function oscilloscope with bandwidth in excess of 80GHz; and an innovative jitter analyzer for electrical and optical signals. It has an electrical bandwidth to over 80GHz to ensure the most accurate waveforms for signals from 50Mb/s to 40 GB/s and beyond. The optical module covers from 155Mb/s to 40 GB/s with optical bandwidths to over 65GHz for the most accurate waveform fidelity.

15

Figure 11: 12GHz IR Photo Receiver

The IR Photo Receiver in Figure 11 is DC coupled and consists of GaAs PIN photodiodes with GaAs heterojunction-bipolar-transistor (HBT) transimpedance amplifiers.

Figure 12: Tunable Laser Source MG9638A

The Tunable Laser Source in Figure 12 uses a semiconductor amplifier providing a high-power output at least -15dBm to 8dBm. Wavelength: 1520nm-1570nm.

16
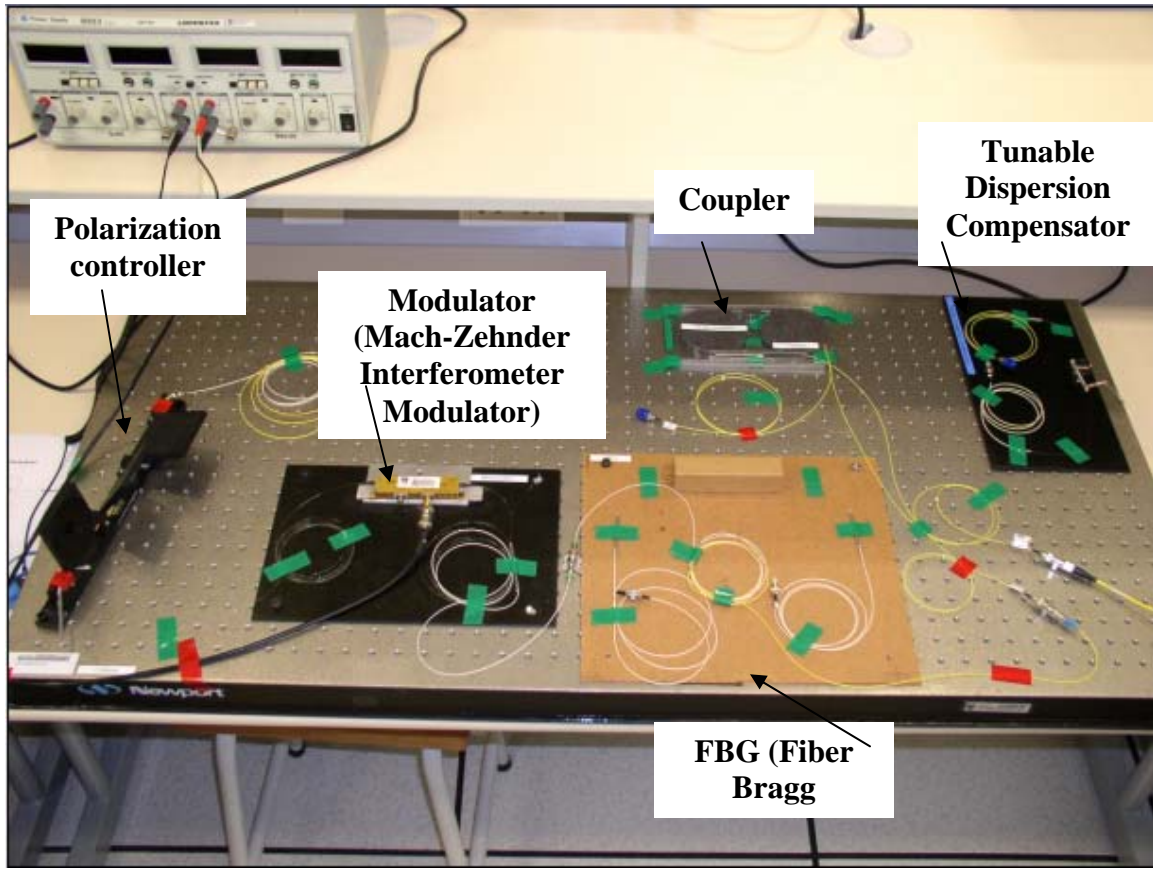
Figure 13: Experimental Setup

Figure 13 shows the experimental setup that was experimented on in the summer. Optical devices are very sensitive and prone to damage, therefore these experimental setups and the equipments used have to be handled with care. Hence when handling the modulator, an anti-static strap has to be worn; optical connectors have to be covered with a cap and are wiped with methanol before a connection is made. Besides all connectors are to be hand tightened only as additional force might cause damage.

Figure 14: Mach-Zehnder Interferometer Modulator

Figure 14 shows the MZIM used in the experiment.

Figure 15*: Polarization Controller*

The polarization controller in Figure 15 has the ability to change the polarization mode of the light within the fiber. Its main usage is to change the polarization before connecting to a polarization sensitive device such as the MZIM. For normal operations, this device is configured with 2 turns, 4 turns, and 2 turns of fiber. Polarization controllers can be easily implemented to convert elliptically polarized light from single mode fiber into linearly polarized light. It's as simple as coiling a prescribed number of fiber loops into each paddle, and adjusting the three paddle positions. These polarization controllers utilize stress-induced birefringence to create three independent fractional "wave plates" to alter the polarization of the transmitted light on single mode fiber. The fiber is looped into three independent spools, creating three independent fractional "wave plates" (fiber retarders). The amount of birefringence induced in the fiber is a function of the fiber

18

cladding diameter, the spool diameter (fixed), the number of fiber loops per spool, and the wavelength of the light.

Figure 16: Coupler

A coupler is made by fusing 2 fibers together and continuously checking the output of the coupler, stopping when the desired effect is achieved. This device was used to split the optical signal for connection with separate testing instruments.
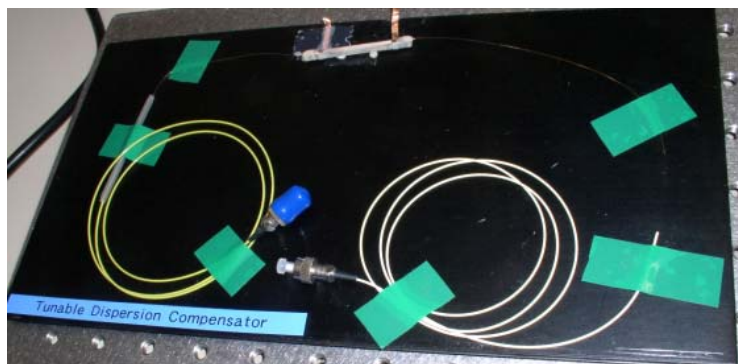
Figure 17*: Tunable Dispersion Compensator*

The tunable dispersion compensator shown above was used to tune the chromatic dispersion qualities of the optical signal.

3.2. Experimental Results

3.2.1   Observation of the sidebands of the MZIM

The following experiment was conducted on the modulator. The aim of this experiment was to identify the sidebands on the frequency spectrum. The modulating frequencies are generated with sinusoidal waveforms at 3.3GHz, 4.3GHz, 5.3GHz, 6.3GHz, and 7.3GHz. The sidebands from the modulating frequencies were visible due to the high resolution of

19

the Optical Spectrum Analyzer as seen in Figure 4. The same simulation was also attempted using MATLAB SIMULINK, however the results were not as ideal as problems were faced when attempting to increase the resolution of the spectrum scope provided in MATLAB SIMULINK.

The observation that was made from this experiment was when the modulation frequency was increased; the sidebands occur further away from the carrier frequency. When working with optical systems, the carrier frequency is determined by the wavelength of the chosen laser source. From the following frequency spectrums, it can be observed that the particular laser source that was used for this experiment was tuned to 1510nm.

| (a) | (b) | (c) |
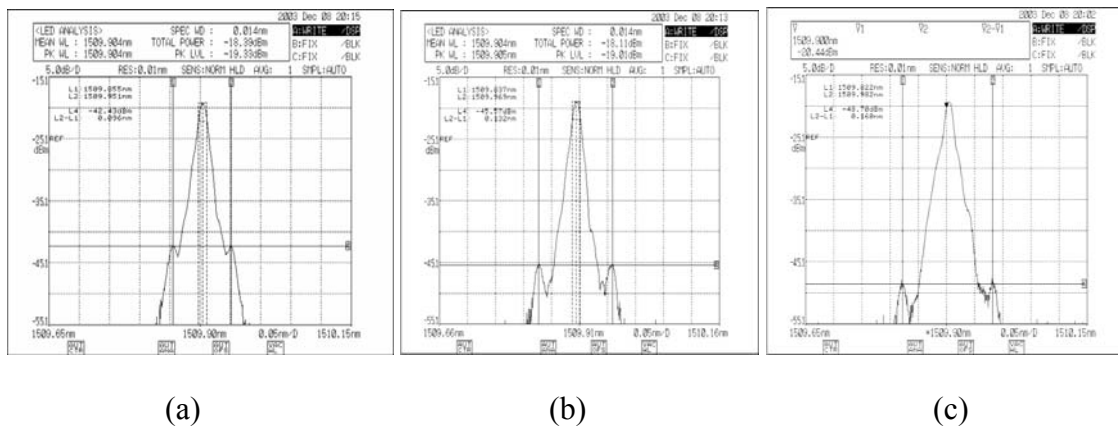
Figure 18: Frequency spectrum generated with (a) 3.3 GHz sinusoidal waveform (b) 4.3 GHz(c) 5.3 GHz .

| (a) | (b) |

20
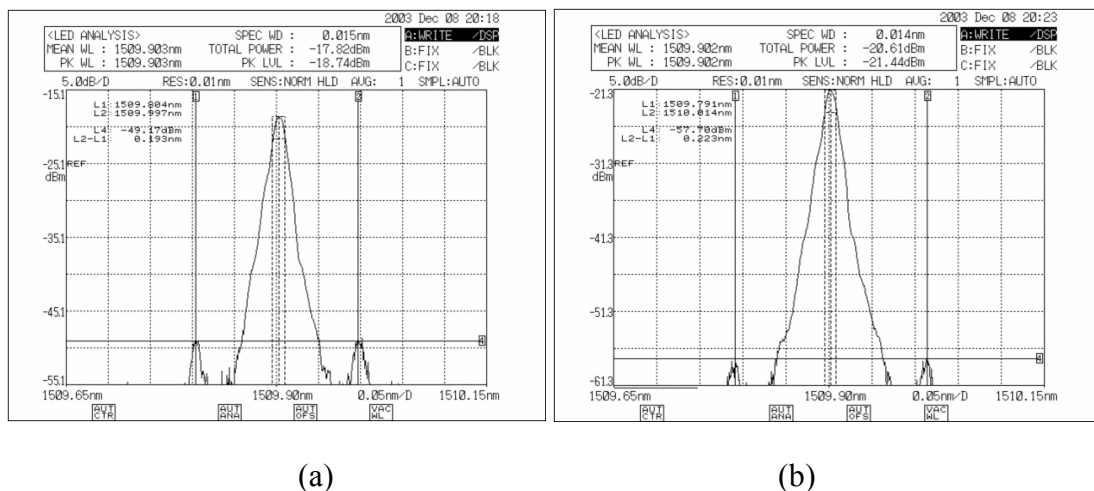
Figure 19: Frequency spectrum generated with (a) 6.3 GHz sinusoidal waveform (b) 7.3 GHz.

From Figure 18 it can be observed that in reality the carrier wavelength is not a spike but a spread of frequencies with a center at a wavelength of 1509.9nm. From Figure 19, with a modulating frequency of 6.3 GHz the sidebands lie at 1510nm and 1509.8nm. If this signal were to be transmitted through a SMF of sufficient length; the sideband at 1510nm will propagate slower than the sideband at 1509.8nm. This will probably result in distortions at the receiving end of the fiber. Considering further the effects, when a pulse is to be modulated, the spread of harmonics would be modulated as well. A pulse is made up of sinusoids at different frequencies; hence this spread of harmonics would be propagating through the fiber at differing speeds.

3.3. The V_{bias} of the MZIM

The next experiment was conducted to find the V_{bias} of the MZIM modulator. By varying the voltage and noting the corresponding power, the results were plotted in the graphs shown in Figure 20 (a) and (b).
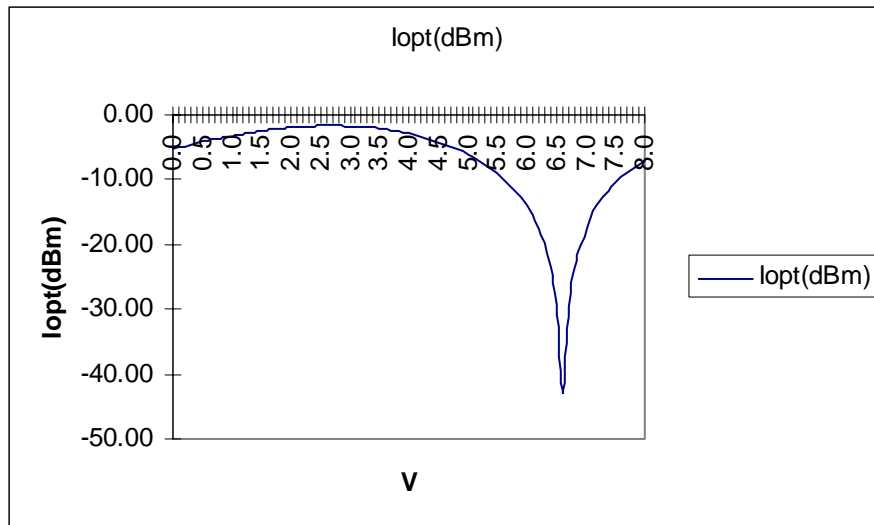
(a)
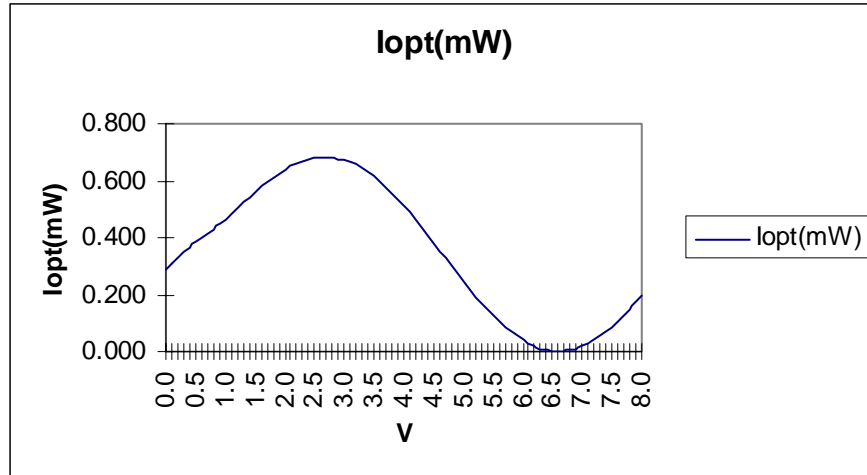
(b)

Figure 20: Measured MZIM characteristics (a) Driven voltage versus power in dBm (b) in linear scale.

With the experimental results of this MZIM in Figure 20, these understandings are modeled in the simulator to be described in the next sections.
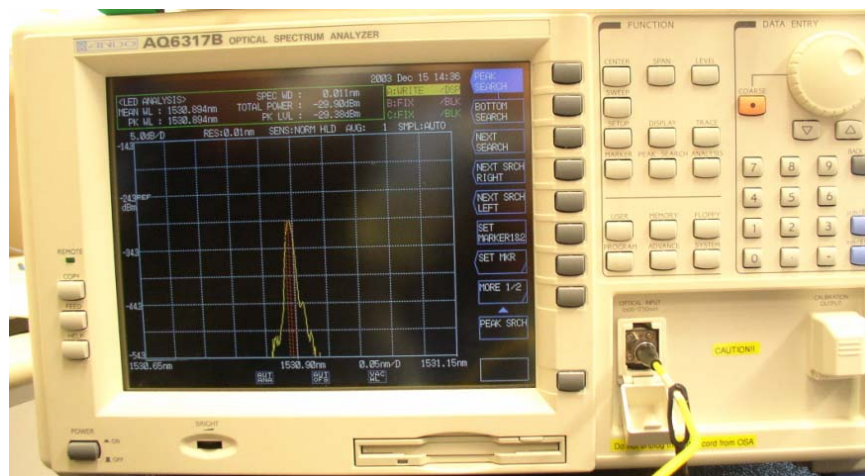
Figure 21: *Frequency spectrum to observe the carrier frequency*

From the frequency spectrum as seen in Figure 21, at a Vbias of 6.5V, it was found that it was the point of lowest output power of -50.28dBm.

MONASH
UNIVERSITY
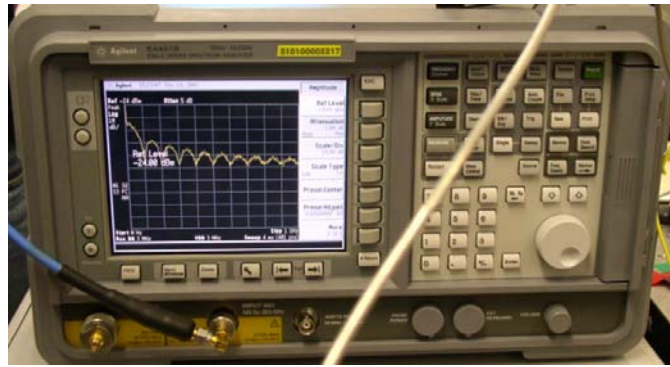
Figure 22: Electrical Spectral Analyzer used to observe the modulating frequencies

As seen in Figure 22, the Electrical spectral analyzer shows the spectral analysis of the sidebands. This spectrum analyzer was set to a span of 0 to 500 MHz.

3.3.1 The BER of the MZIM

Another experiment was conducted to find the Bit Error Rate (BER) for the Modulator. The objective of this experimental setup was to see the Eye-Diagram and to measure the bit-error. The T-joint is removed to minimize the errors and the input is taken directly into either the Signal Analyzer or the Bit Error Detector. The experimental setup is as follows:

<u>Back to Back</u>

Before proceeding with the transmission experiment, a test set was used to test if the output from the optical amplifier was below 5dBm. The reason is that the photo-detector required to convert optical signal to electrical signal can only operation between -5 dBm to 5 dBm.
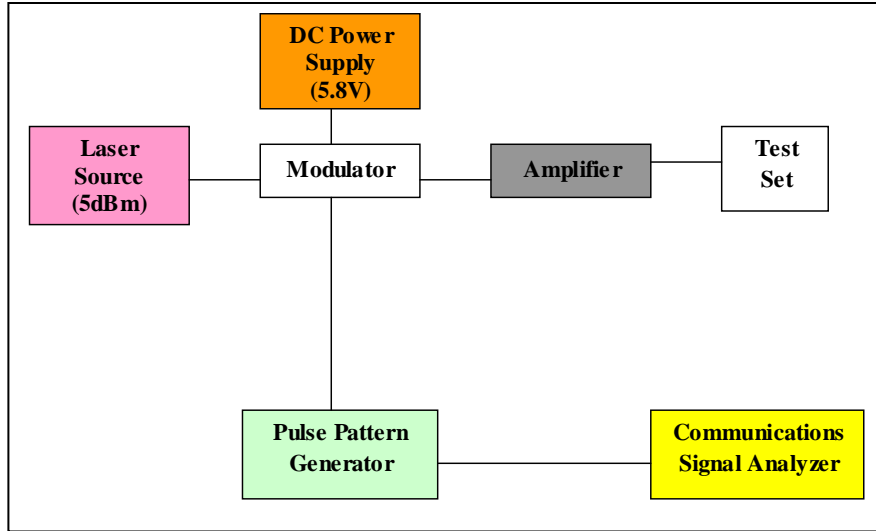
Figure 23: Experimental setup to check if input output of optical amplifier is between -5dBm and 5dBm before feeding into Photo-detector.

After ensuring that the output from the optical amplifier is within the operating range of the photodetector, the following experiment as observed in Figure 24 was set up. The actual experimental setup without fiber:
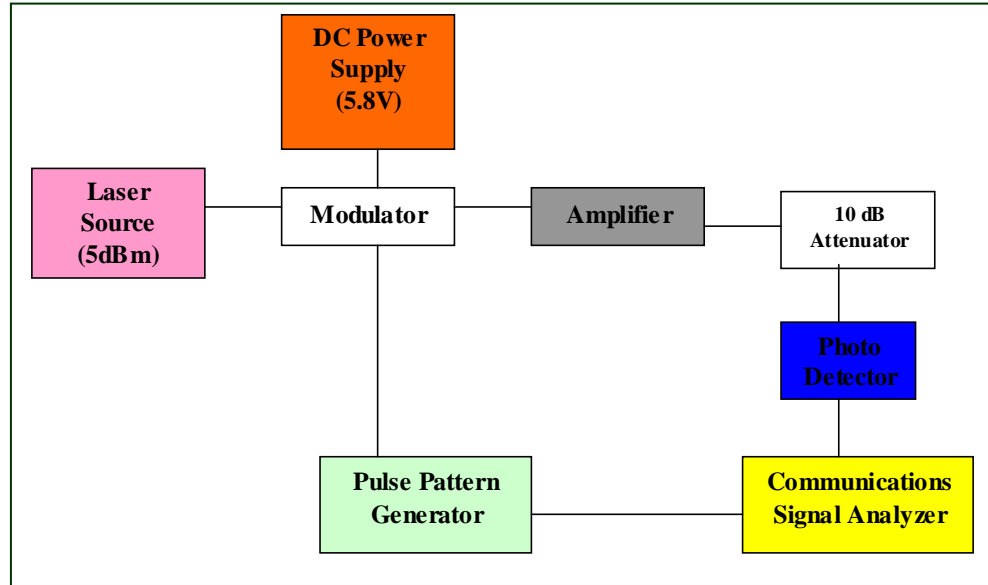
(a)
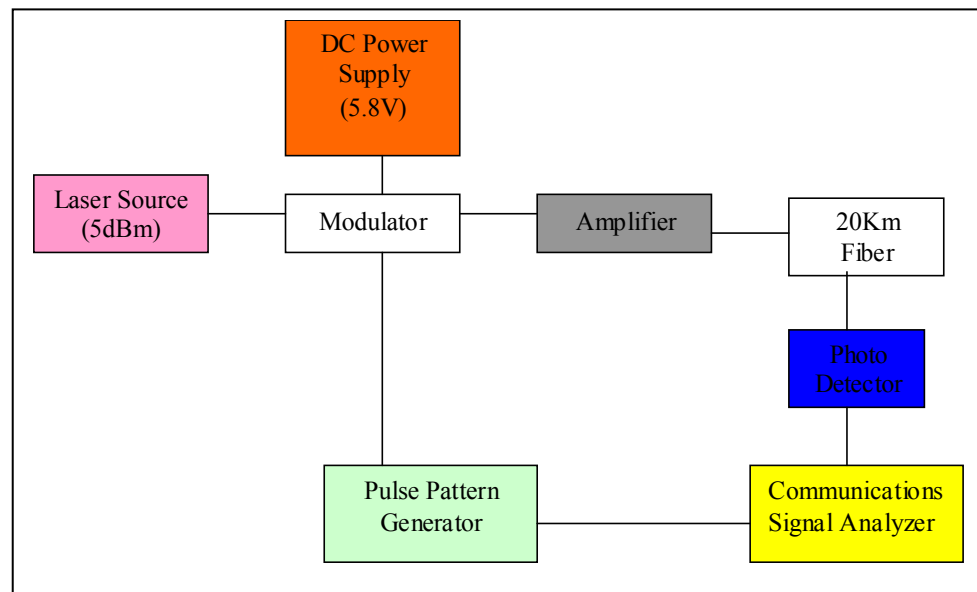
(b)

Figure 24: Experimental setup to measure the BER of the MZIM(a) without fiber.(b)

with 20km of fiber.

Transmission Results:
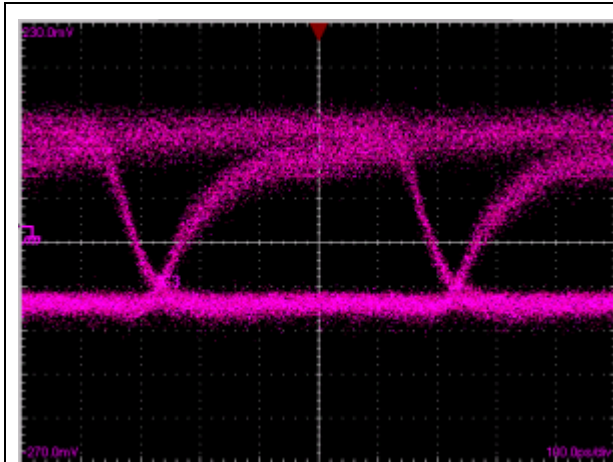
Q-Parameter: 1.8/0.3 = 6; BER = 10^{-12}
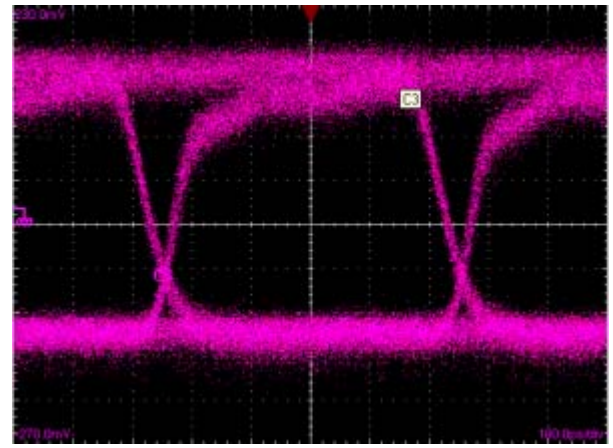
Q-Parameter: 2.8/0.4=7; BER = 10^{-12}

Figure 25(a) 2Gb/s with fiber   *(b) 2 Gb/s without fiber*
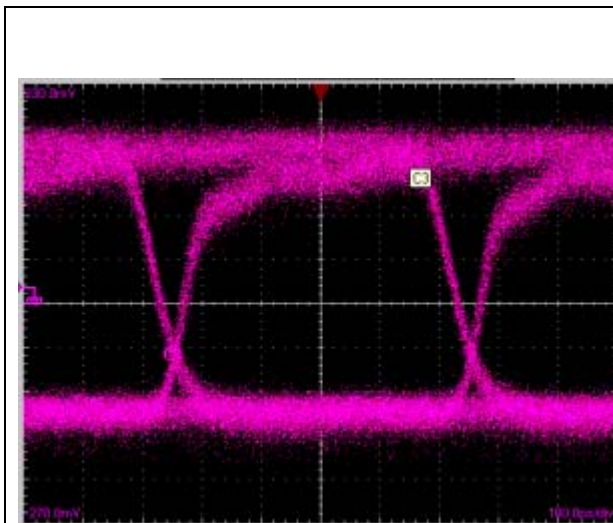
Q-Parameter: 2.4/0.4 = 6; BER = 10^{-9}
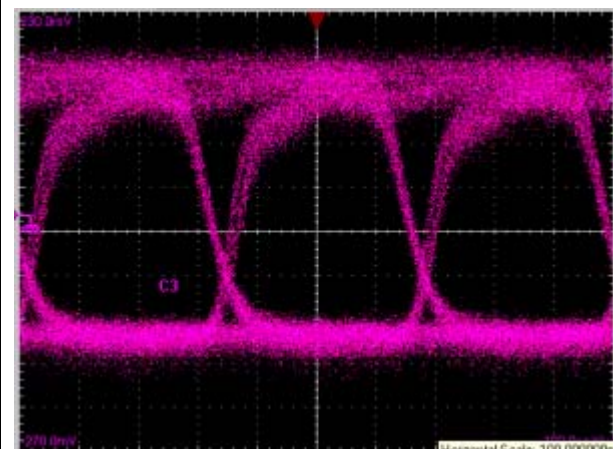
Q-Parameter: 2.8/0.4 = 7; BER = 10^{-12}

Figure 26(a) 3Gb/s with fiber   *(b): 3 Gb/s without fiber*
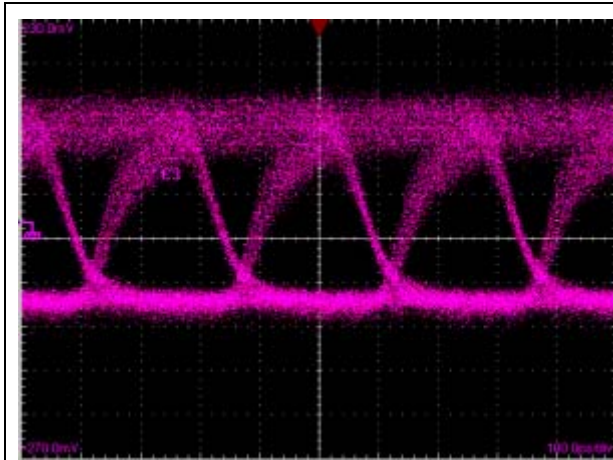
Q-Parameter: 1.8/0.3 = 6; BER = 10^{-9}
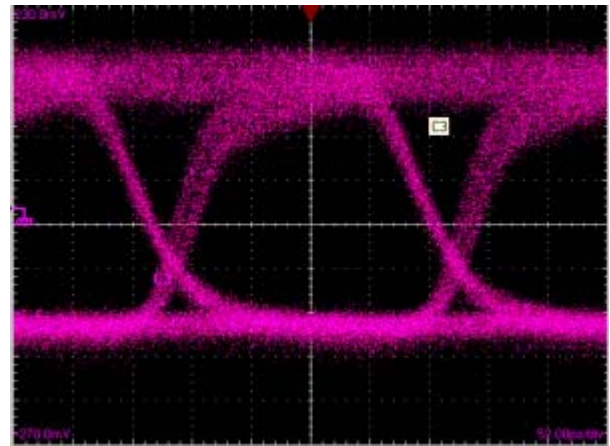
Q-Parameter: 2.8/0.9 = 7; BER = 10^{-12}

Figure 27(a) 4 Gb/s with fiber   *(b) 4 Gb/s without fiber*
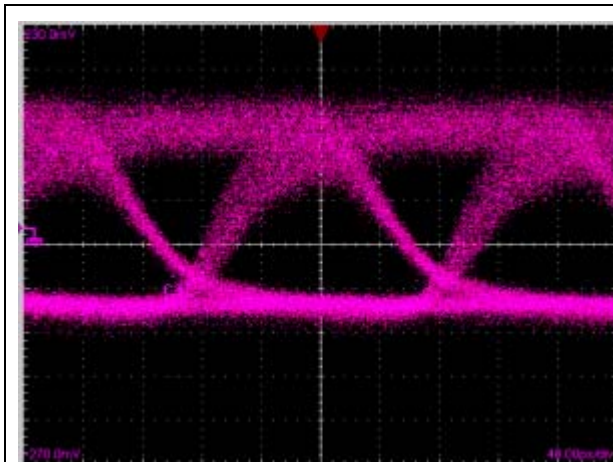
Q-Parameter: 1.5/0.25 = 6; BER = 10^{-9}
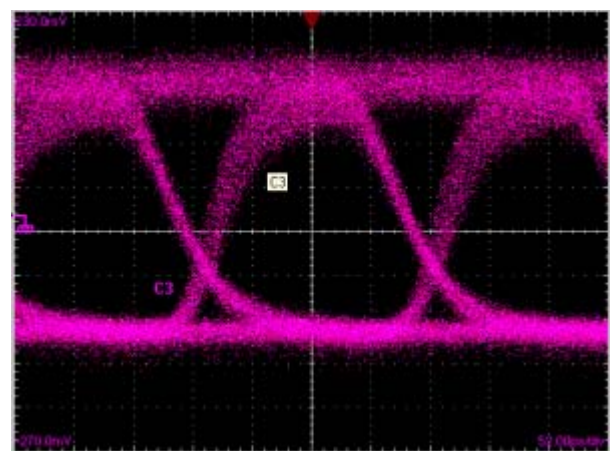
Q-Parameter: 2.45/0.35 = 7; BER = 10^{-12}

Figure 28(a) 5 Gb/s with SSMF   *(b)5 Gb/s without fiber*

| Q-Parameter: $1.5/0.25 = 6$; BER $= 10^{-9}$ | Q-Parameter: $2.25/0.22 = 7$; BER $= 10^{-12}$ |
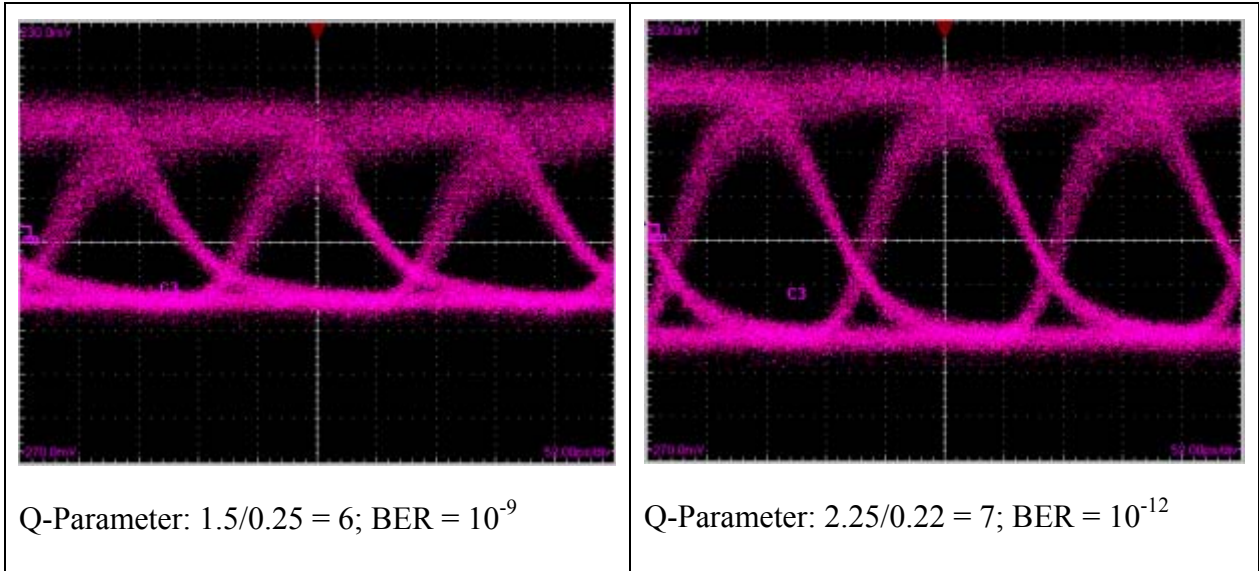
Figure 29(a) 6Gbps with fiber   (b) 6Gbps without fiber

| Q-Parameter: $1.2/0.2 = 6$; BER$=10^{-9}$ | Q-Parameter: $2.3/0.35=6.6$; BER$=10^{-11}$ |
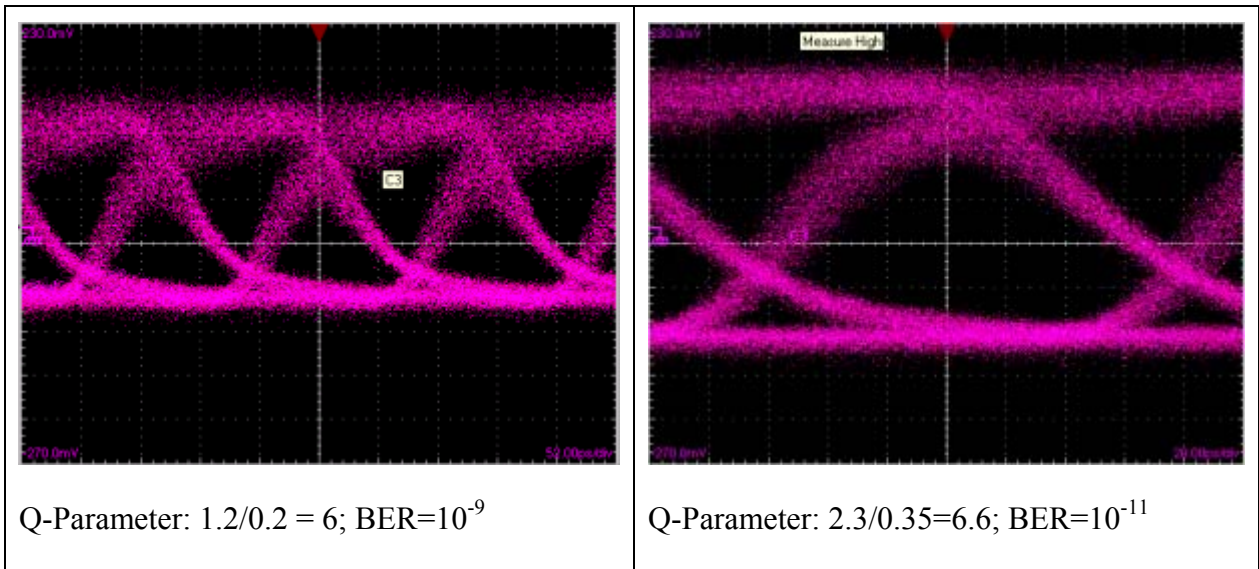
Figure 30(a): 7Gb/s with fiber   (b): 7Gb/s without fiber
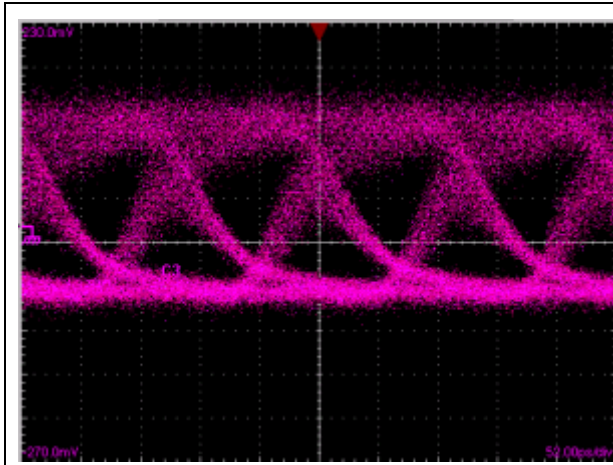
Q-Parameter: 0.9/0.25 = 3.6; BER = 10^{-5}
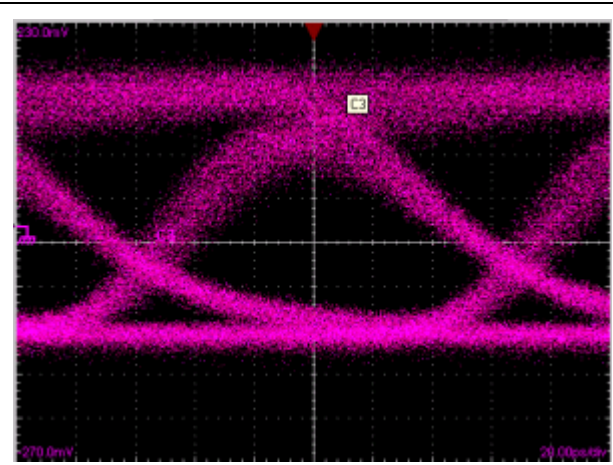
Q-Parameter: 2.1/0.4=5.3; BER=10^{-8}

Figure 31(a) 8 Gb/s with fiber   *(b): 8 Gb/s without fiber*
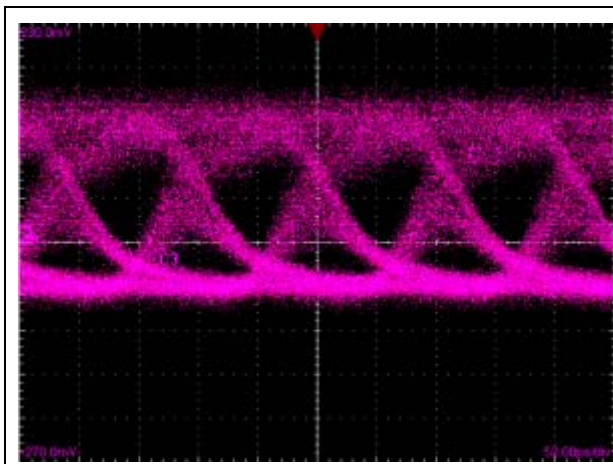
Q-Parameter: 0.5/0.3 = 1.6; BER = 10^{-2}
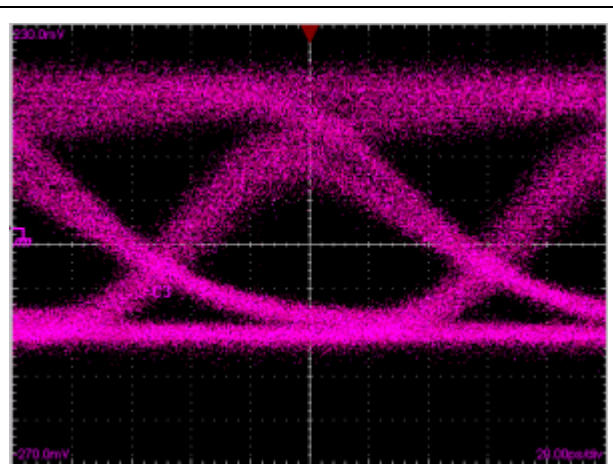
Q-Parameter: 1.7/0.4=4.25; BER=10^{-6}

Figure 32(a): 9 Gb/s with fiber   *(b): 9 Gb/s without fiber*

29

Q-Parameter: 0.4/0.4 = 1; BER = 10^{-1}

Q-Parameter:1.7/0.4=4.25; BER=10^{-6}
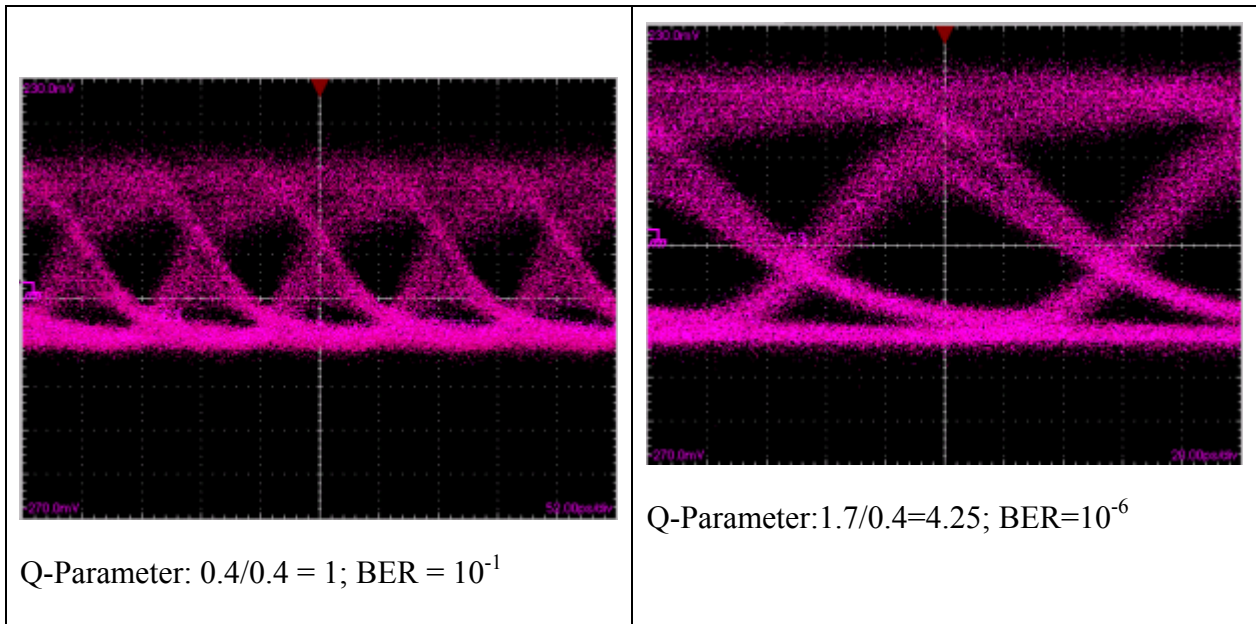
Figure 33(a) 9.5 Gb/s with fiber   (b) 9.5Gb/s without fiber

A typical target for telecommunications and data transmission is 10^{-12} (one error in a trillion bits). The significant difference in BER between Figure 25 and Figure 33 was expected and can be attributed to the chromatic dispersion associated with the transmission medium (SMF) which causes pulse broadening. It is observed that, as the bits per second increases the BER increases. This effect can be attributed to the effects of chirp on the MZIM.   The increase in bits per second also increases the harmonic frequencies needed to create the pulse. This effect is the same as increasing the modulating frequency, the spread of the spectrum increases. Due to the effects of the SMF fiber, increasing the spread of the spectrum has a negative effect on the chromatic dispersion of the fiber, causing higher dispersion if not compensated, as in our case. To estimate the BER, let consider the eye diagram of *Figure 34*.

MONASH
UNIVERSITY

Figure 34: An eye pattern[2]

The BER is estimated by using $Q = \dfrac{\mu_1 - \mu_0}{\sigma_1 + \sigma_0}$ where: $\sigma_1 = 0.68\bar{\sigma}_1$ and $\sigma_0 = 0.68\bar{\sigma}_0$ for

Gaussian pulses. Thence when Q=6, BER=10^{-9} and Q=7, BER=10^{-12}.

4. The SIMULINK SIMULATOR

4.1. *Design Process*

This simulator prototype was completed using MATLAB SIMULINK. The first prototype that was designed in MATLAB SIMULINK was the Non-return to Zero Transmitter from the experimental setup. The first stage of that design was signal modulation, where the signal is modulated with 2 sources, a sine generator, and a random binary generator. The next stage involved in designing the voltage bias function block. The MATLB SIMULINK model has been modeled based on system experiments; therefore this voltage bias function block was designed based on the experimental results and graphs obtained for the 10G/bits MZIM.

The last stage is the fiber propagation model which is designed using the linear phase model of a low pass filter (LPF). This fiber propagation model is fitted into this MATLAB SIMULINK model.

31

Four different format (as listed above) transmitters are then subsequently designed in MATLAB SIMULINK. The transmitter models are then integrated with the fiber propagation model and the receiver models to study the system performance.

4.2. NRZ Transmitter

4.2.1 Non-Return to Zero (NRZ)

NRZ-OOK is the most widely deployed modulation format in optical communication systems. This modulation format outputs data on an optical carrier by switching the light signal on and off. External modulation is considered in this design as directly modulated laser light is highly chirped and will broaden the optical spectrum and hence degrade transmission performance. Hence for long haul optical communication systems, external modulation is usually used. As mentioned in previous section, an experiment has been conducted employing a $LiNbO_3$ MZIM external modulator. For the transmitters that were designed, the carrier frequency is scaled down to $100*10^9$ Hz. The carrier *c(t)* is a pure sinusoidal signal given by:

$$c(t) = A_c \cos[2\pi f_c t + \theta_c(t)] \qquad\qquad \textbf{(2)}$$
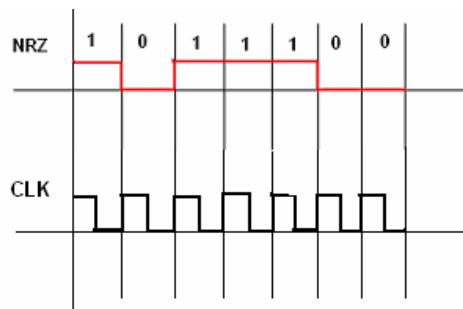
Figure 35: Representation of the NRZ code

A Simulink block diagram is shown in *Figure 36* which is based on the earlier development [4] but for a back-to-back testing.

32
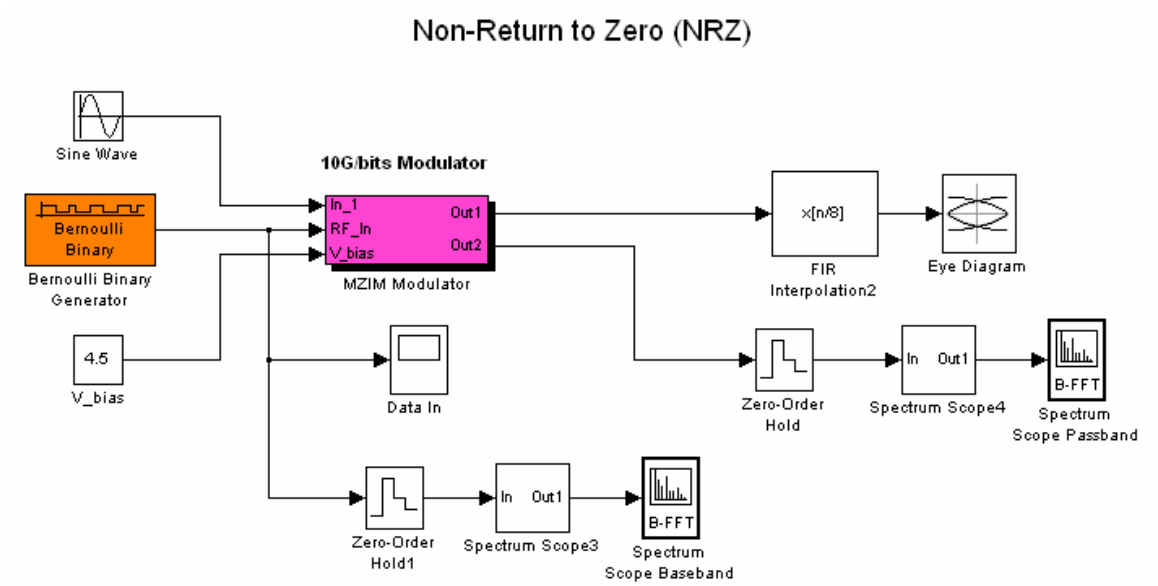
Figure 36: SIMULINK model of the system- back-to-back configuration.
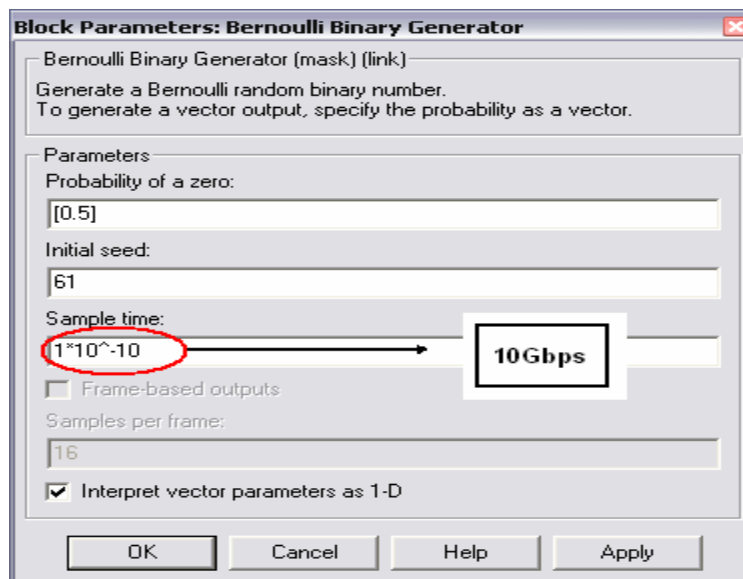
Figure 37: Parameters of the Bernoulli Binary Generator.
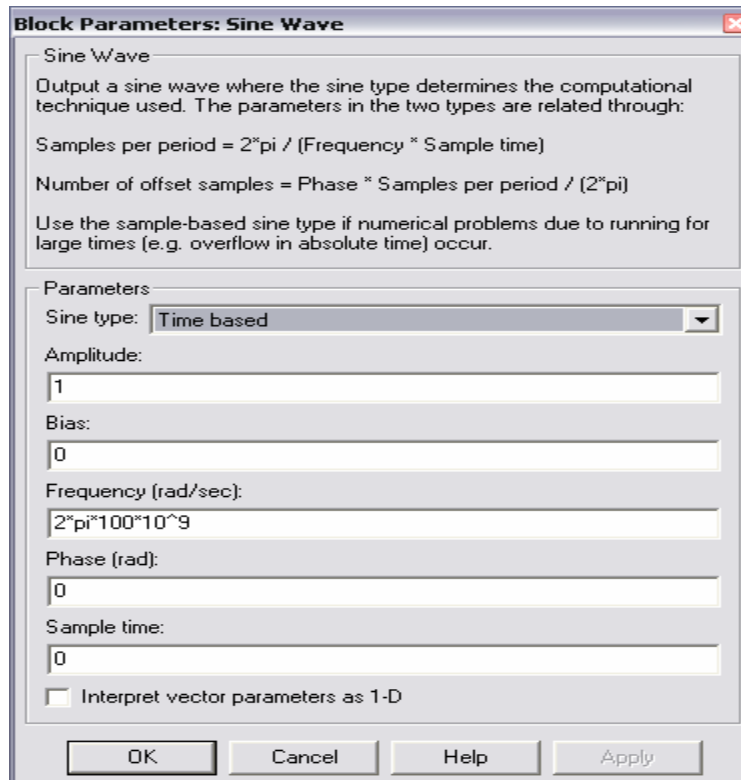
Figure 38: Parameters of the carrier

To produce the carrier signal, the sine wave with a frequency of $2\pi*100$ GHz is set; where 100 GHz is the carrier frequency. The up scaling to the optical carrier at 1550 nm can be implemented with ease.

4.2.2   10G/bits MZIM block
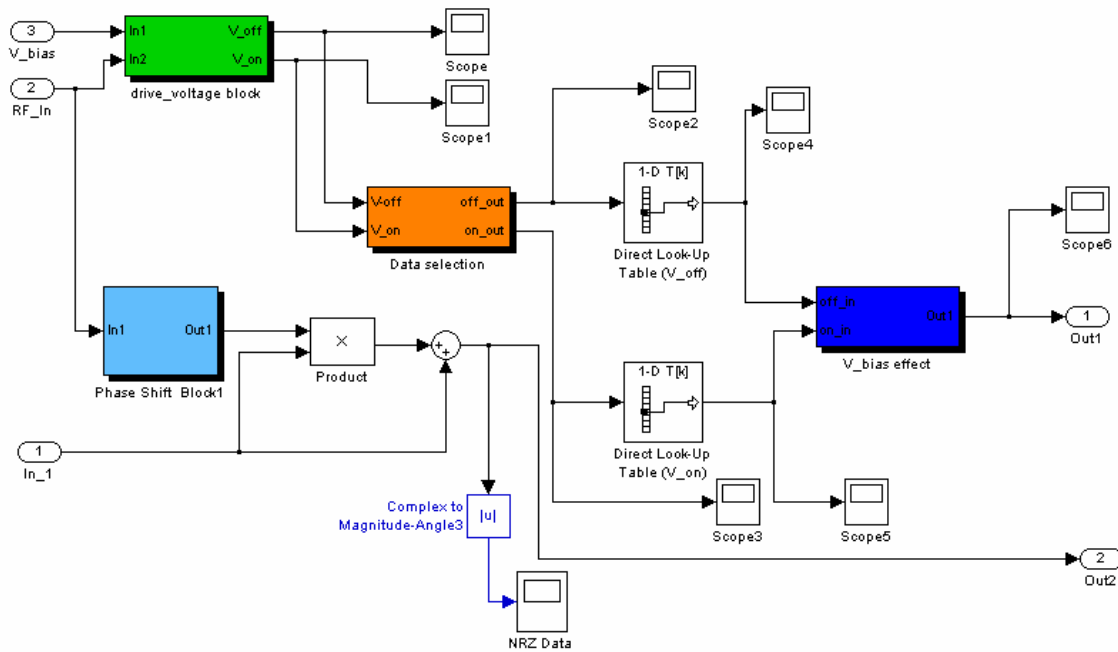
Figure 39: Inside the 10G/bits MZIM block.

Figure 39 shows the 10 Gb/s MZIM block of the system. The Voltage bias of the modulator is a very important parameter as the voltage biasing point would directly affect the output optical strength of the signal. Hence a separate sub-system was designed. The sub-systems in the MZIM block include:

- The *drive_voltage* block was designed to select the V-bias range set by the driving voltage. Where the driving voltage here refers to the voltage strength of the RF signal (Refer to Figure 40).

- The data selection block that would interpret the modulation transfer curve as a numerical table of the actual experimental values.

- The *V_bias* block output the effects of the selected Voltage Bias point. This output would be produced as a percentage of the optical signal intensity that would either reduce or maximize the modulated signal output.

These three blocks are modeled according to the MZIM characteristic curve in Figure 40. The phase shift block in arm two of the MZIM causes a 0 degree phase shift if the input

35

signal was a '1' bit, hence resulting in zero phase shift and producing the 'ON' state when it recombines with the signal from arm 1. If the input signal was a '1' bit, there will be a phase shift of π hence causing the signals to cancel out and when they recombine with the signal from arm 1, hence causing the 'OFF' state.
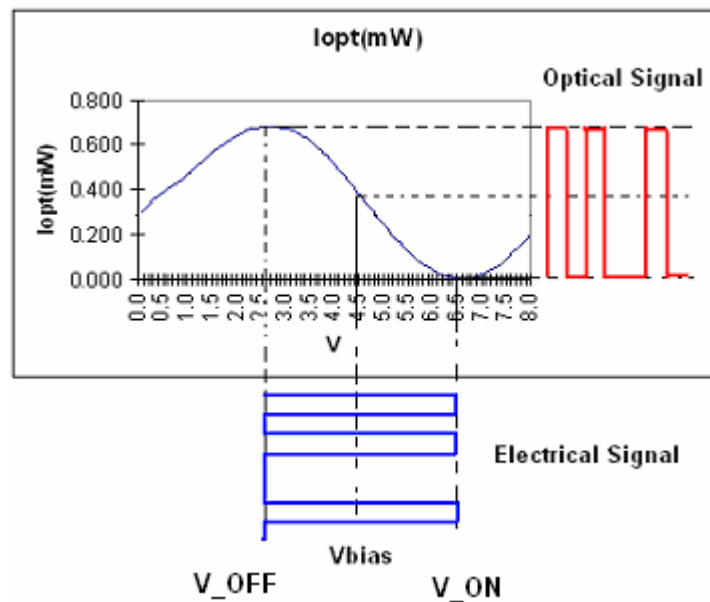
Figure 40: MZIM characteristic curve

4.2.3   RF Voltage block
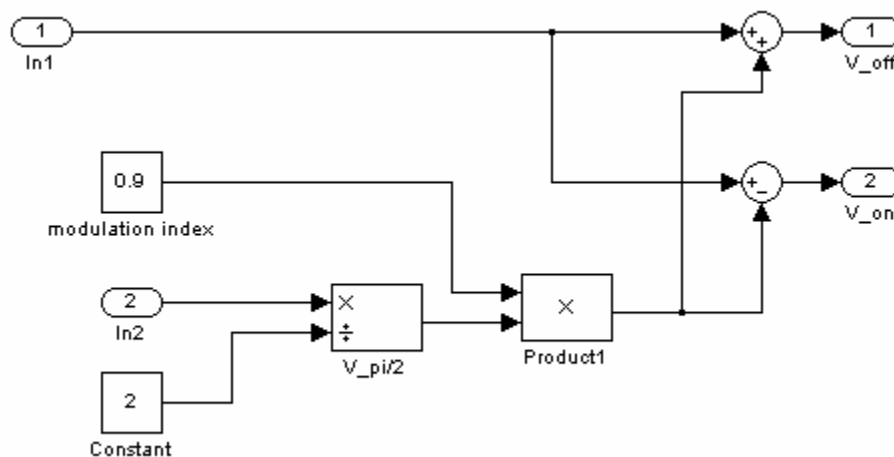
Figure 41: Inside the drive voltage subsystem.

In the drive voltage block (*Figure 41*), the voltage level of the 'ON' and 'OFF' signals from the MZIM characteristic curve in Figure 40 can be generated.

4.2.4 Data Selection block
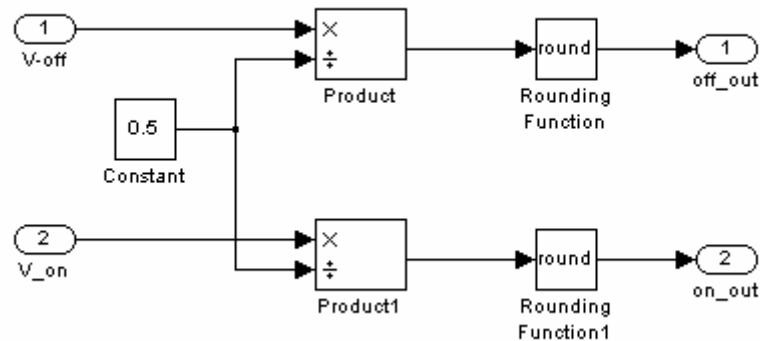
Figure 42: Inside the data selection block

To model the MZIM, the measured transfer characteristic curve of the MZIM is used. The data selection block as shown in *Figure 42*is incorporated with the direct look-up tables of the transfer characteristics. The output intensity and optical phase at the output of the modulator can be determined.

4.2.5 V_bias Effect Block
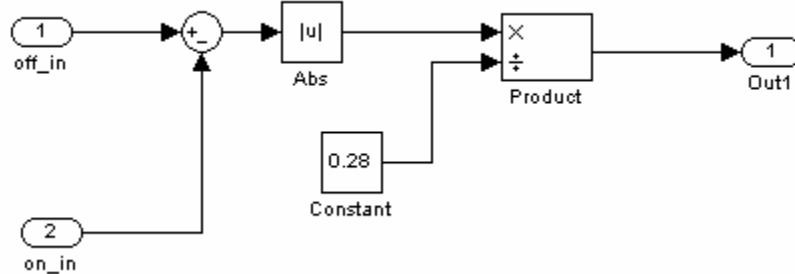
Figure 43: Inside the V-bias effect block

The V_bias block as shown in *Figure 43*is then used to generate the total output intensity of the simulated modulator.

4.2.6   Results

Figure 44 shows the input data from the Bernoulli generator and Figure 45 shows the resultant OOK signals. Comparing the two scopes, we can see that Figure 45 produces a NRZ data format with the carrier component after the MZIM. *Figure 46* and *Figure 47* show the optical spectra of the signals.
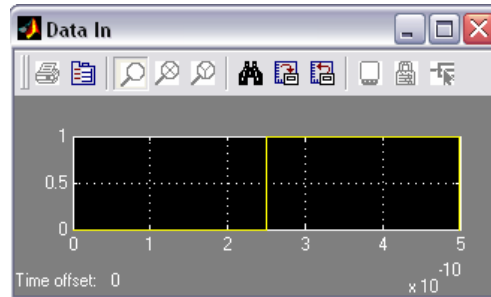
Figure 44: Scope displaying the data from the Bernoulli Binary Generator.
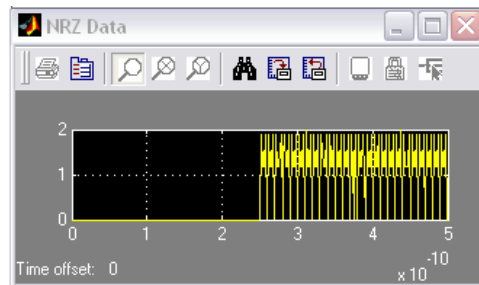
Figure 45: Scope displaying the modulated signals with carrier.
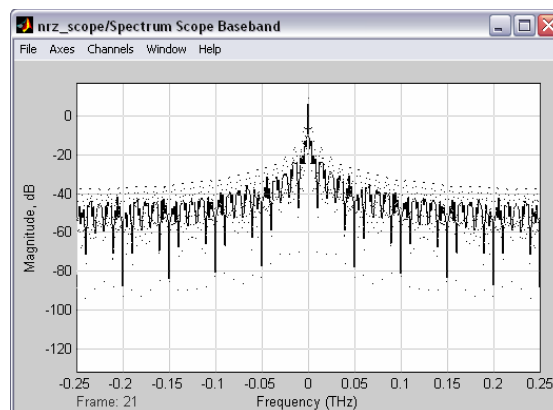
Figure 46: Spectrum scope observed with the centre of the optical carrier frequency shifted back to the baseband.

38

Comparing Figure 46 and Figure 47, it can be observed that at passband, the carrier is assumed an artificial value of 0.1 THz by setting the carrier frequency of the signal generator block. Indeed this is the advantage of employing Simulink for simulation as it can illustrate the optical waves that would not be possible to observe in practical system.
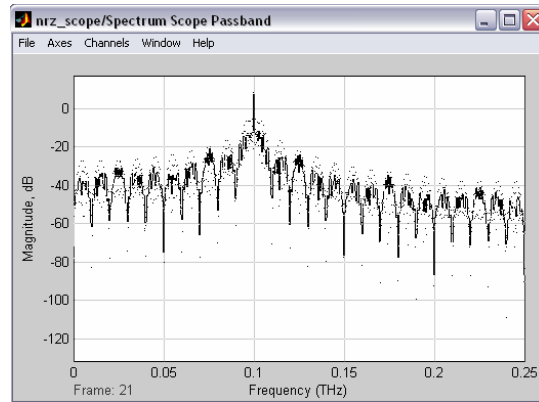
Figure 47: Spectrum Scope observed at passband
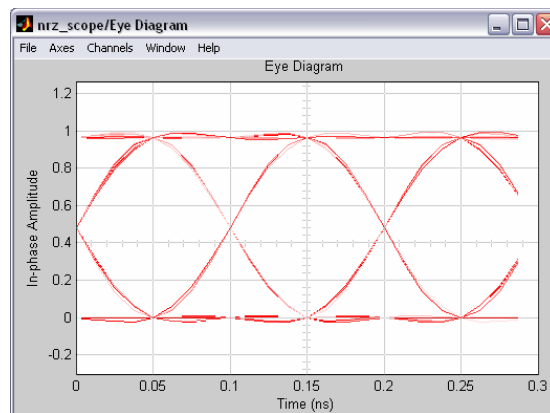
$$BER = 10^{-12}$$

Figure 48: Electrical Eye-Diagram observed at 10 Gb/s

The eye-diagram is measured at 10 Gb/s and a $BER = 10^{-12}$ or error free is obtained.

4.3. *NRZ-OOK Transmitter with 80km Single Mode Fiber (SMF) and Dispersion Compensation Module (DCM)*

After modeling the NRZ transmitter, the fiber propagation model is incorporated into the model. The fiber propagation model is designed using both the split step Fourier method[5] and a low pass filter approach which would be reported in another part of the series. The fiber propagation model has a total length of 80 km SSMF and incorporating a

39

Dispersion Compensation Module (DCM). The eye diagrams are measured at the input and output of the fibre. The DCM has a total dispersion of -1360 ps/nm at 1550 nm and dispersion slope of 0.01 ps/nm.
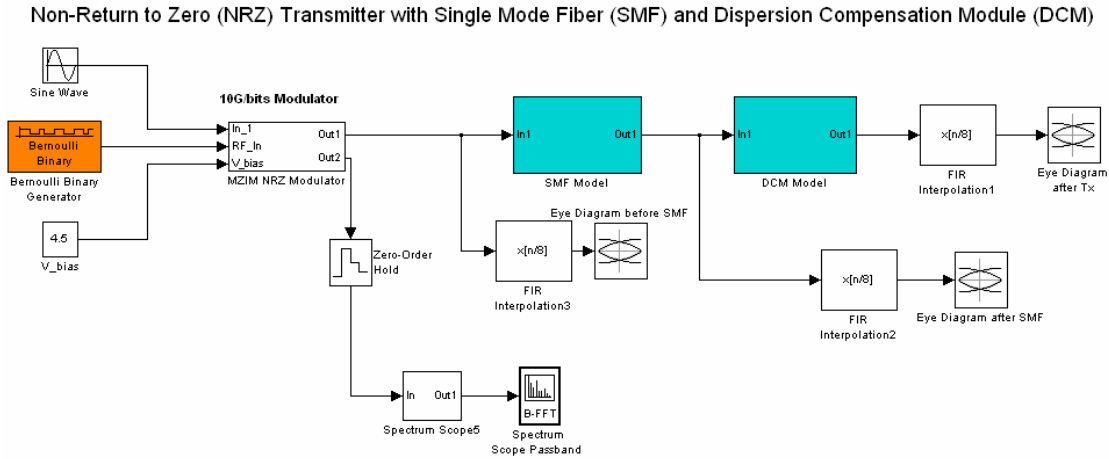
Figure 49: MATLAB SIMULINK model of the optically amplified system using SMF and DCM.
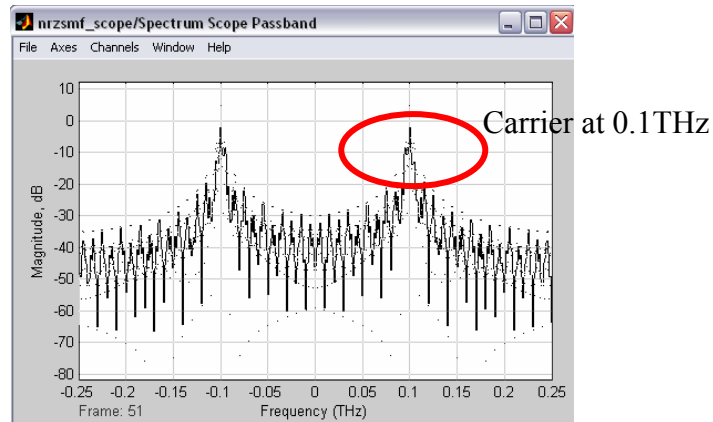
Figure 50: Spectrum scope observed before the SMF

$BER = 10^{-12}$
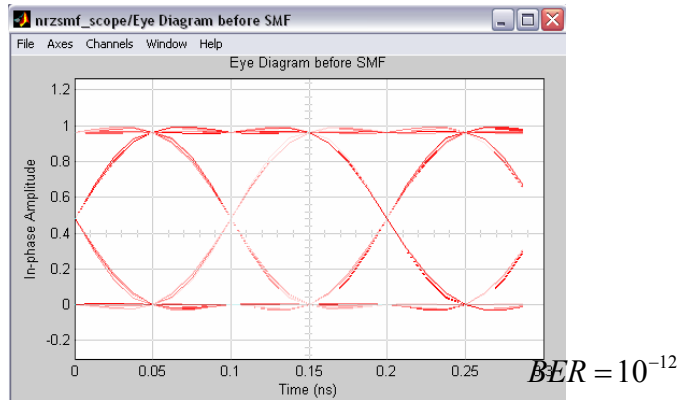
Figure 51: Eye Diagram in electrical domain of the NRZ transmitter observed before the SMF

$BER = 10^{-5}$
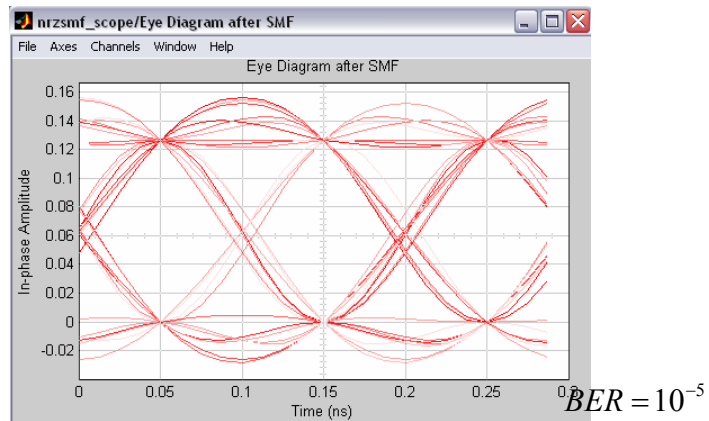
Figure 52: Eye Diagram in electrical domain of the NRZ transmitter observed after the SMF

Comparing the eye diagrams of Figure 51 and Figure 52, it can be observed the BER is 10^{-5} after 80 Km transmission due to the attenuation and dispersion effects of the fiber. After the DCM, the eye-diagram observed in Figure 53 has achieved an error free with a $BER = 10^{-12}$. This demonstrates the effectiveness of the simulator.

41

$$BER = 10^{-12}$$
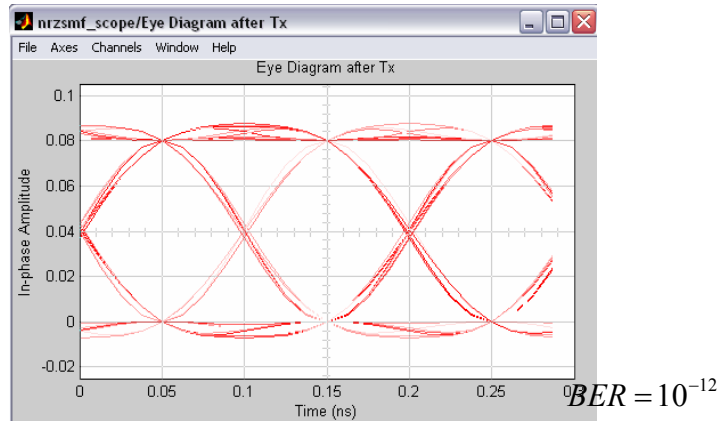
Figure 53: Electrical Eye Diagram of the NRZ transmitter after a 80 km span ofS SMF and DCM

4.4. NRZ-OOK Transmitter with 80km Dispersion Shifted Fiber (DCF)

Another fiber propagation model consisting of 80 km of Dispersion Shifted Fiber (DSF) is also incorporated with the NRZ transmitter. The eye diagrams before and after the fiber are observed and the BER is measured.
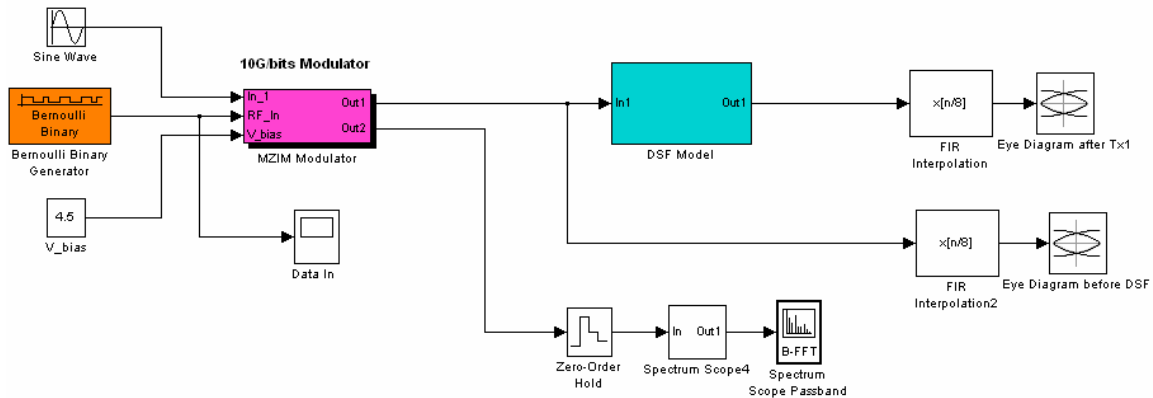
Figure 54: SIMULINK model of the system in Singapore with DSF.
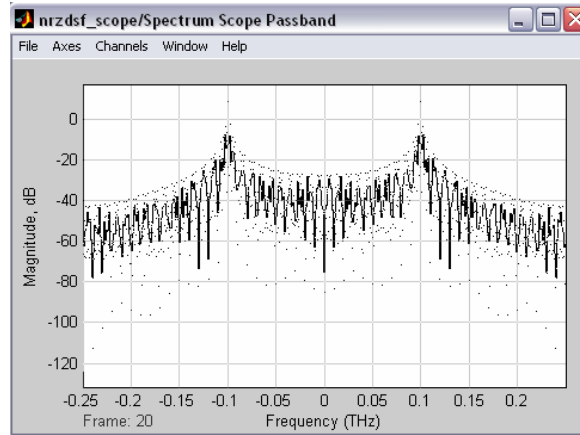
Figure 55: Spectrum scope observed before the DSF

$BER = 10^{-12}$
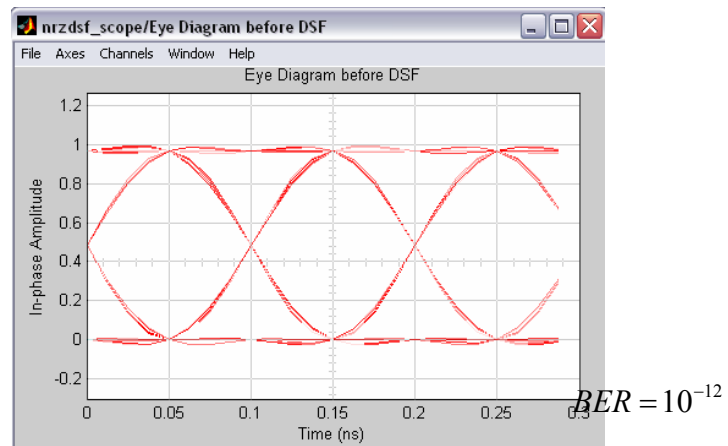
Figure 56: Electrical Eye-diagram observed from the scope before the DSF fiber

$BER = 10^{-12}$
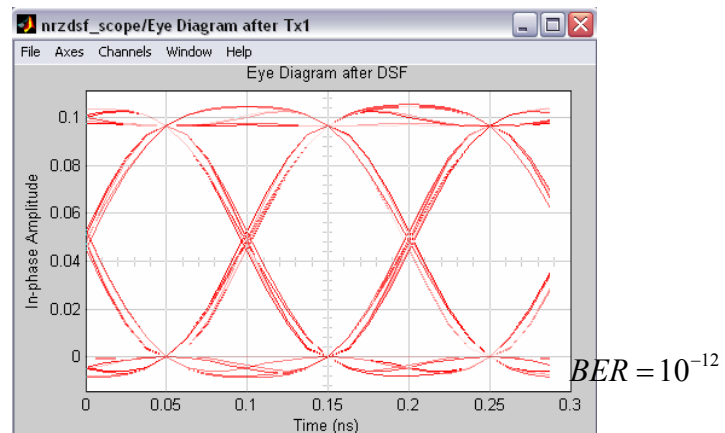
Figure 57: Electrical Eye diagram observed from the scope after the DSF

Comparing Figure 56 and Figure 57, it can be observed that after the DSF span, the eye-diagram is significantly closer due to the attenuation of the DSF span. However minimum dispersion is observed due to low dispersion of the DSF. The simulator thus demonstrates the simulation of the NRZ transmitters together with the fiber propagation models, the effects of the linear dispersion, the fiber non-linearity and attenuation of fibers.

4.5. NR-OOK Transmitter with Demodulation

Modulation is the technique of superimposing the message signal, *m(t)* on the carrier at the transmitter. At the receiver end, demodulation has to be done to receive the original that was transmitted. The concept of modulation and demodulation is illustrated in Figure 58(a) and (b). *Figure 59* shows the Simulink simulator

(a)   (b)
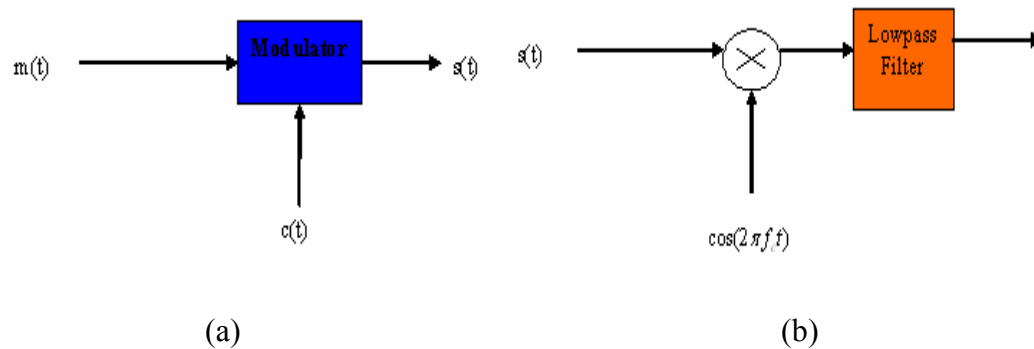
Figure 58: Block diagram of (a) modulation and (b) demodulation
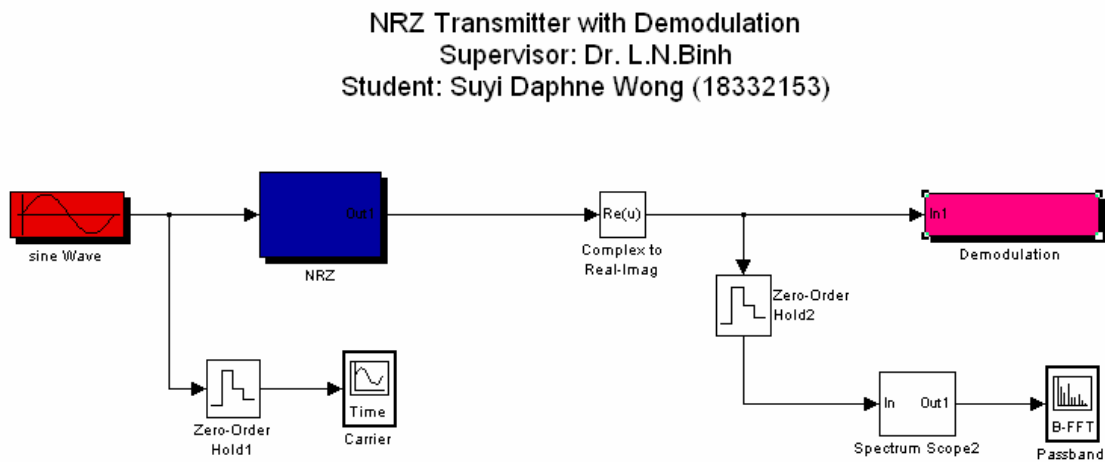
Figure 59: MATLAB SIMULINK model of the NRZ transmitter with demodulation.

44

4.5.1 NRZ block

In the NRZ block, the carrier signal is fed into the MZIM. As explained earlier, the MZIM has two arms. In arm 2 of *Figure 59*, a Bernoulli generator with a sample time of $1*10^{-10}$ (10Gbps) is fed into a phase shift block as referred to in Figure 61. This phase shift block will cause the phase shift in arm 2 of the MZIM. When a '0' bit is received, the phase shift block will cause a phase shift in arm 2, the signal from the two arms will hence be out of phase when they combine and hence canceling out each other and producing zero output intensity; 'OFF' state. When a '1' bit is received, the phase shift block will not cause any phase shift in arm 2 and hence when the signal from the two arms combine, it will produce a signal 'ON' state.
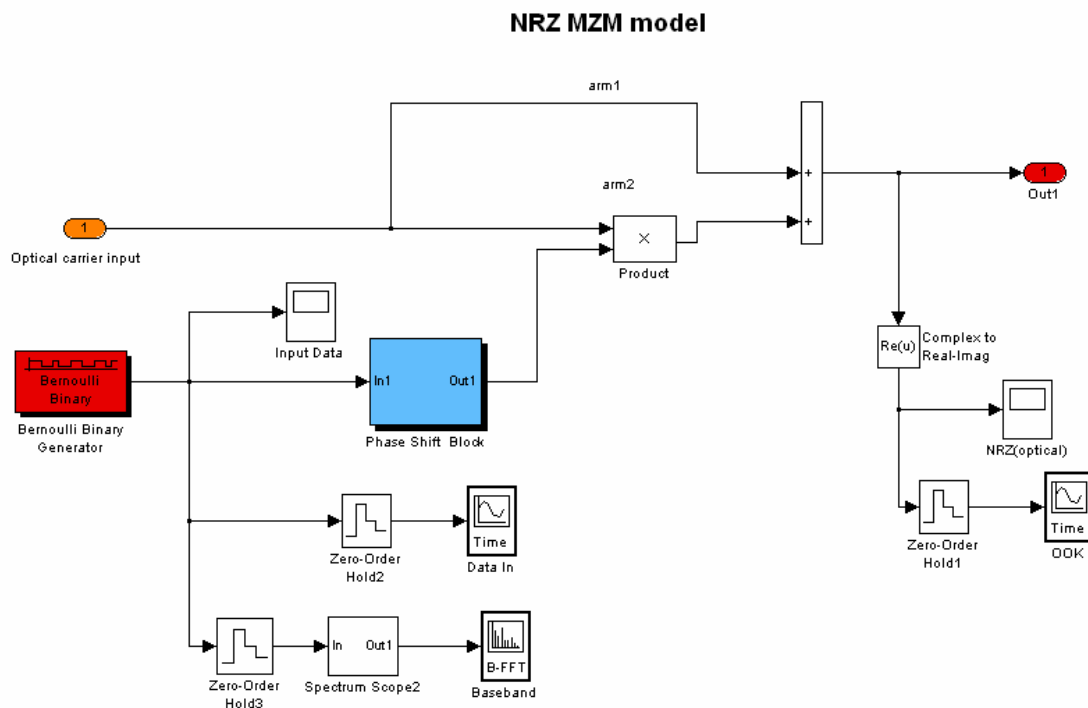
Figure 60: Inside the MZIM block

4.5.2 Phase Shift Block
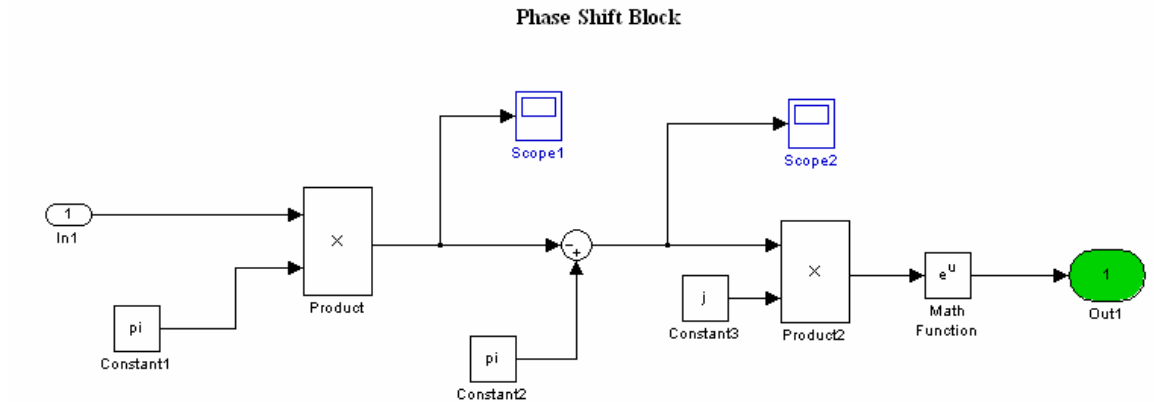
Figure 61: Inside the phase shift block.

The phase shift block will cause a π or zero phase shift in arm2 of the MZIM. When a '1' bit is received; it will be multiplied by π. After which $\pi - \pi$ will produce zero. When multiplied by the complex j and taking its exponential (e^{0j}) will result in a zero phase shift in arm 2 of the MZIM and hence when the signal from the two arms recombine, it will produce a signal; 'ON' state. If a '0' bit is received; it is multiplied by π, after which $\pi - 0$ produces π phase shift. When multiplied by the complex j and taking its exponential ($e^{\pi j}$) results in a π phase shift in arm 2 of the MZIM. Hence when the signal from the two arms recombines; it is out of phase and a destructive interference results, hence producing an 'OFF' state.

4.5.3 Demodulation block

In order for the receiver to receive the data that was transmitter by the receiver, demodulation has to be done. In the demodulation block, the low pass filter excludes the high frequency components and hence producing the demodulated signal as observed in Figure 69.

46
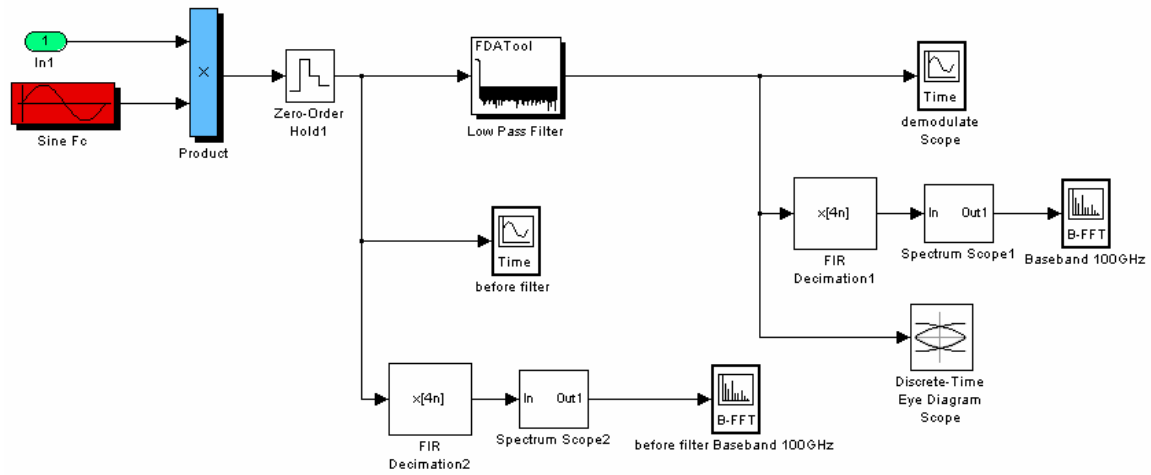
Demodulation

Figure 62: Inside the demodulation block
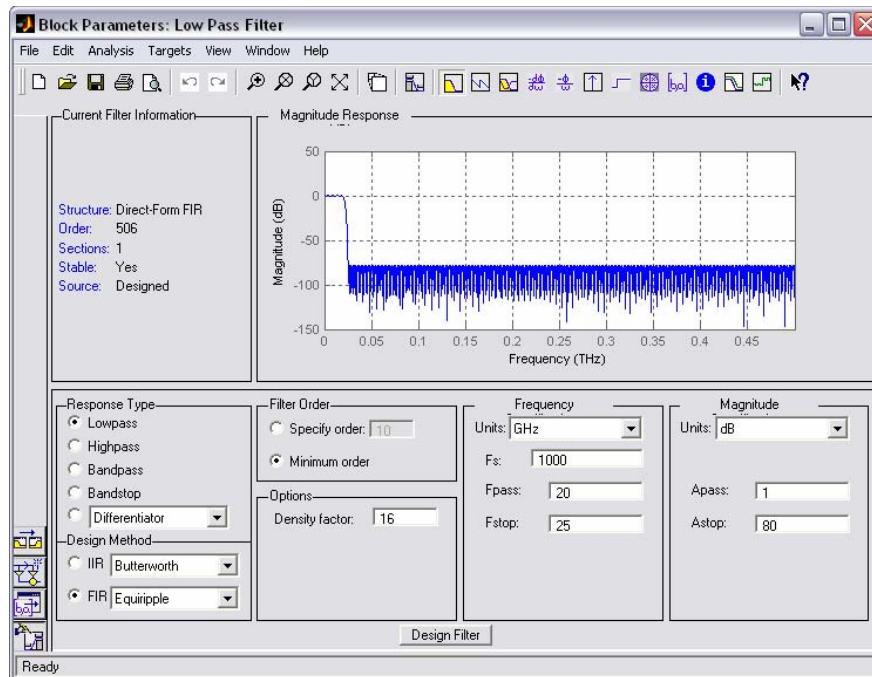
Figure 63: Block parameters of the LPF fiber model.

4.5.4   Results
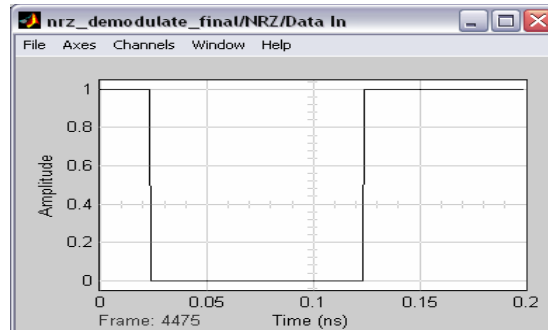
Figure 64: Scope observed at the data input.

Figure 64 shows the data observed at the input of the MZIM, and Figure 65 shows the output observed from the MZIM. Comparing these 2 scopes, it can be seen that after the MZIM, the carrier component can be clearly observed in Figure 65.
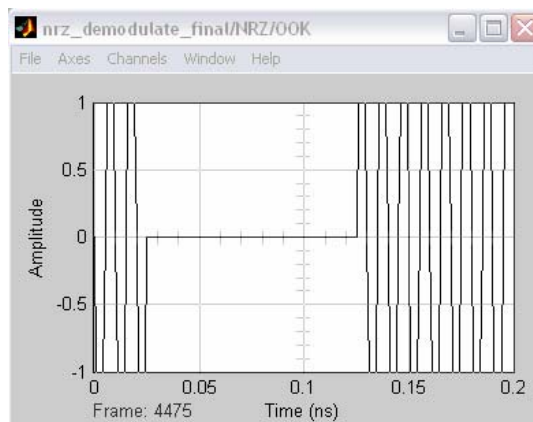
Figure 65: Scope observed after the MZIM.
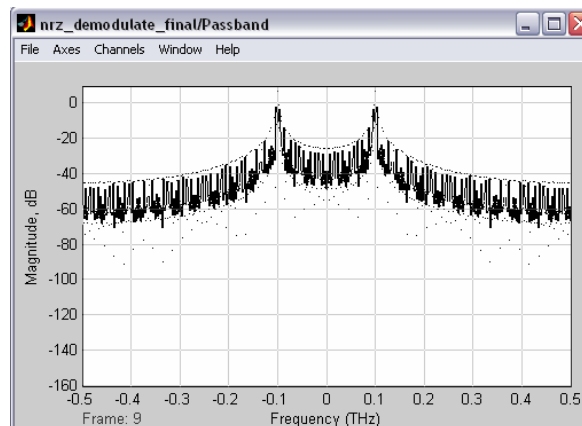
Figure 66 shows that the carrier exists, from the spectrum scope, andlocated at the centre of the passband. It can be seen that the carrier is at 0.1THz as we have initialized at the input to the MZIM. The eye diagram after demodulation can be observed in Figure 67. With a sampling time of 10 Gb/s, the BER of 10^{-12} is measured.
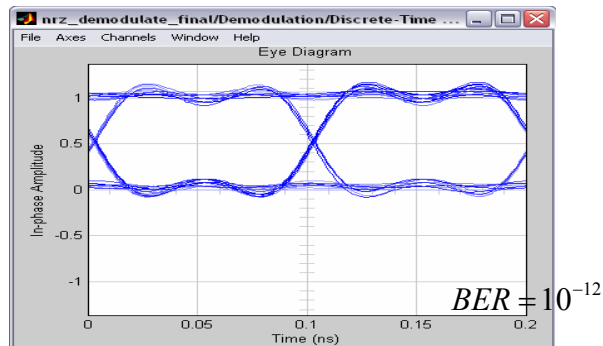
Figure 67: Eye diagram observed at 10Gbps
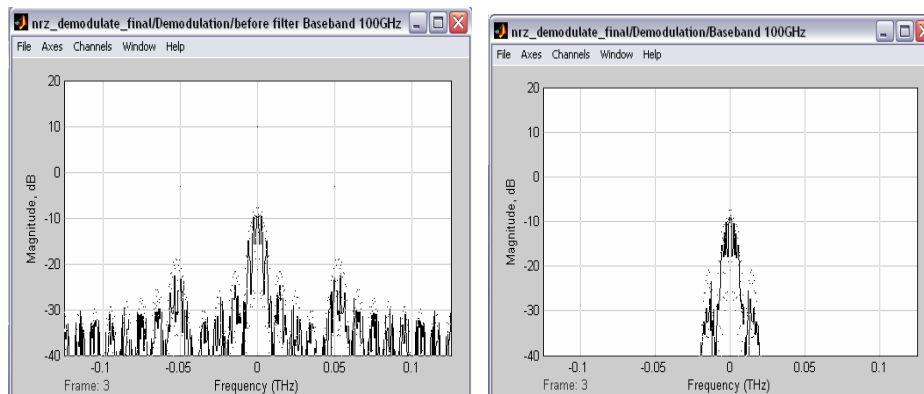
Figure 68: Spectrum scope observed (a) before the low pass filter (b) after the low pass filter

In Figure 68(a), the spectrum scope was observed before the low pass filter. Figure 68(b) was observed after the low pass filter, comparing both scopes, it can be seen that after the low pass filter; the high frequency components were filtered out.
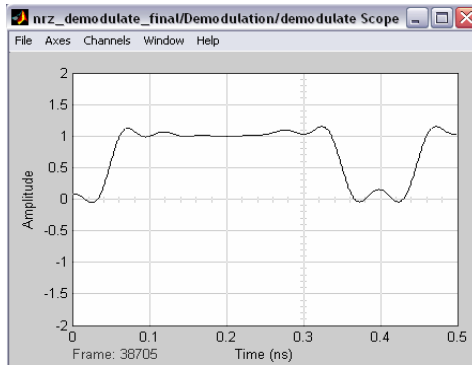
Figure 69: Signal observed after demodulation.

Hence the demodulation scope observed in Figure 69 displays the demodulated signal after the low pass filter (LPF) where the carrier frequency component is removed.

4.6. RZ Transmitter with Demodulation

Return-to-Zero (RZ)

The shortcoming of NRZ is that it often suffers from bandwidth limitations. This will lead to the presence of inter-symbol Interference (ISI) in the detected signal. RZ can minimize problems incurred in NRZ and hence enhance system performance.
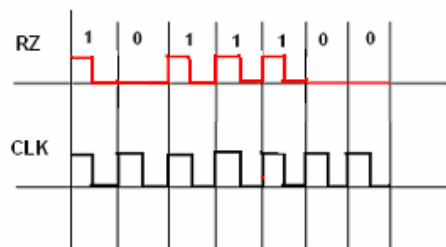
Figure 70: Representation of the RZ code

The design of the RZ transmitter can be modeled using two MZIMs in cascade. The first MZIM acts as a pulse carver or periodic return to zero clock pulses. The second MZIM produces a switching of these periodic pulses according to the ON or OFF states of the data sequence PRBS.

50

RZ Transmitter with Demodulation
Supervisor: Dr. L.N.Binh
Student: Suyi Daphne Wong (18332153)
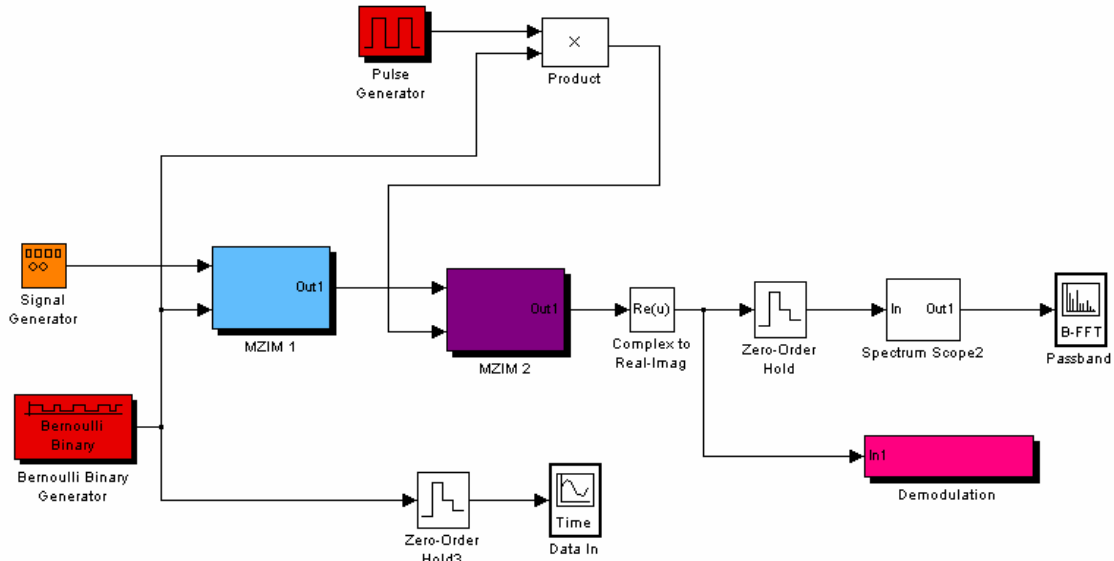
Figure 71: SIMULINK MATLAB model of Return-to-Zero Transmitter model with demodulation

4.6.1 MZIM-2 block

RZ MZM model
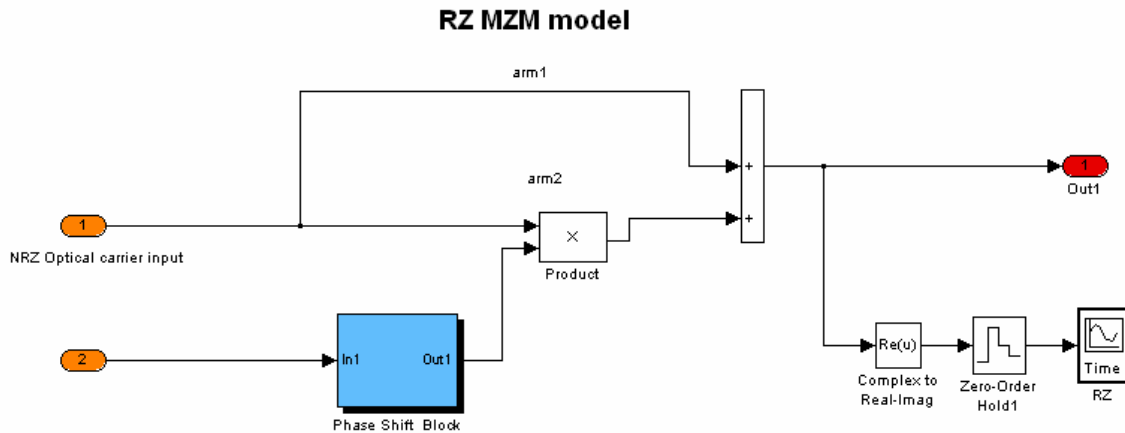
Figure 72: Simulink model inside the second MZIM of the RZ transmitter

In Figure 72, the input port 1 is the NRZ optical signal, and port 2 is the clock pulse generated by a pulse generator. The phase shift block will as explained in section 4.5.2 will phase shift arm 2 of the MZIM block to produce the RZ optical signal.

51

4.6.2 Results

(a)   (b)
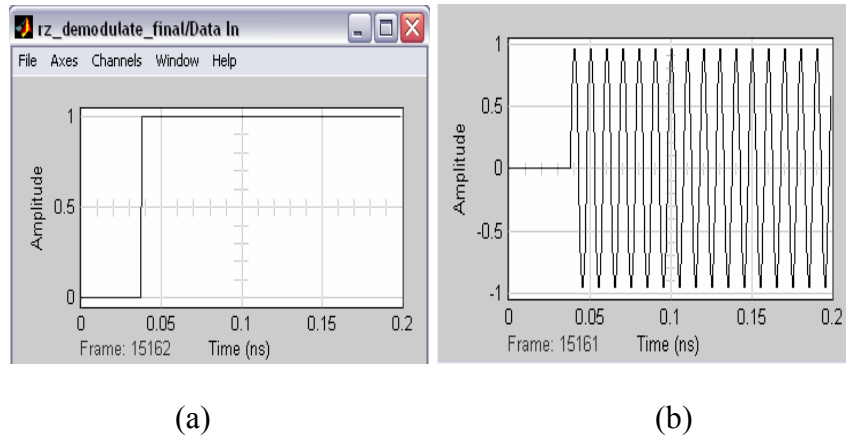
Figure 73: Scope observed (a) at the input (b) after the first MZIM

As observed from Figure 73(b), the carrier is present after the MZIM and the input data to the MZIM can be observed from Figure 73(a).
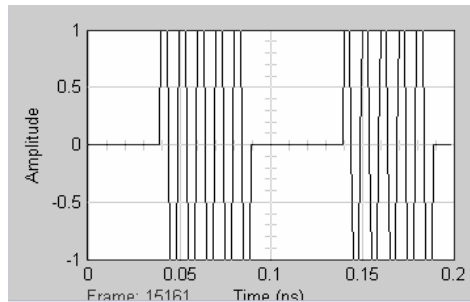
Figure 74: Scope observed after the second MZIM

From Figure 74, it can be observed that after the second MZIM, the output from the second MZIM produces a RZ data sequence as compared to a non-return to zero (NRZ) data observed previously.

MONASH
UNIVERSITY
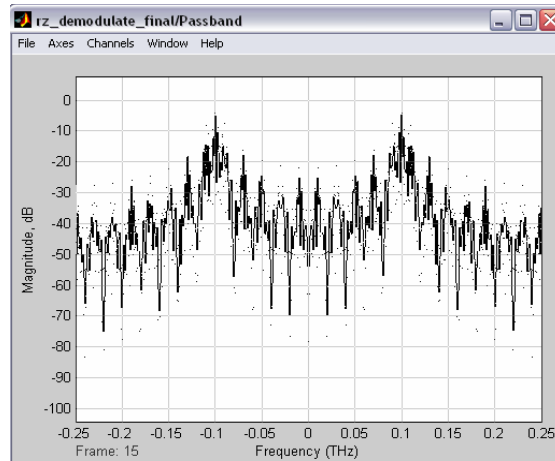
Figure 75: Spectrum scope observed at passband
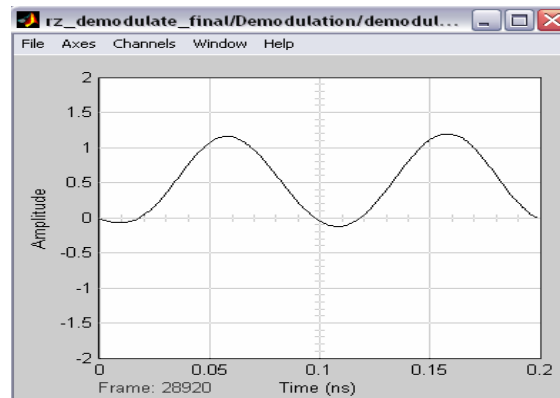
Figure 76: Signal observed after demodulation

Figure 76 shows the demodulated signal after demodulation; it can be observed that the result is a return-to zero data as the pulse width of a received '1' is smaller than the pulse width of a '1' received in a NRZ data in Figure 78.

$$BER = 10^{-12}$$
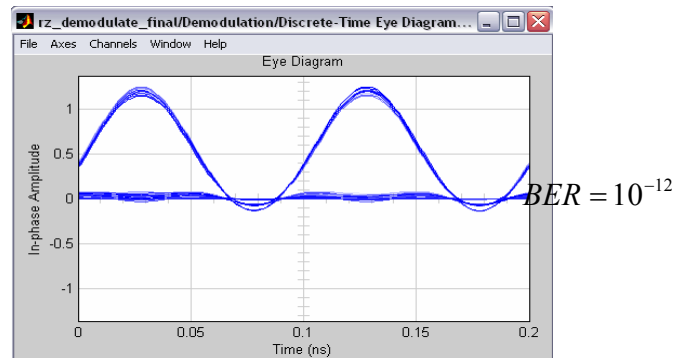
Figure 77: Eye diagram observed at 10 Gb/s
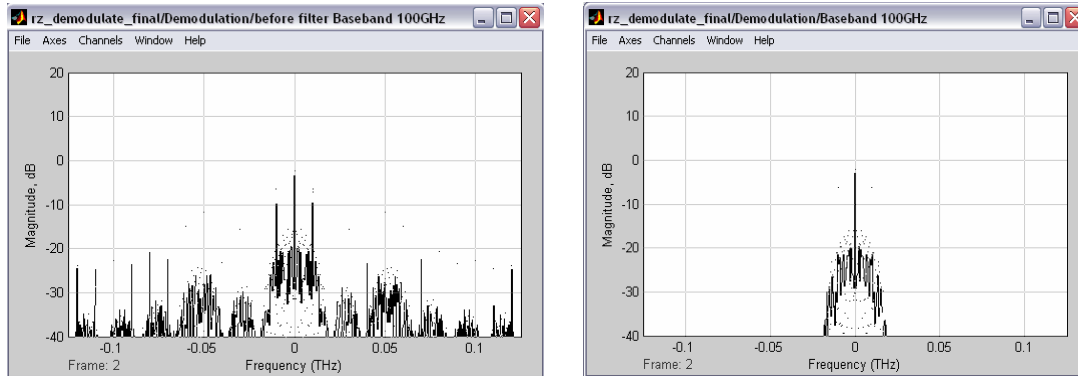
Figure 78: Spectrum scope observed (a) before the low pass filter (b) after the low pass filter

4.7. NRZ DPSK Simulator Model

Differential Phase-Shift Keying (DPSK)

Differential Phase Shift Keying or DPSK modulation signal records changes in a binary stream. Changes in bits will result in a π phase shift.
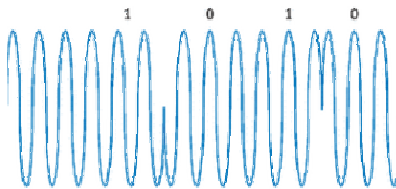
Figure 79: DPSK signals[6]

Phase-shift keyed signals cannot be detected incoherently as they use coherent detection[7]. A coherent detector has two inputs for which one is a reference signal and the other is the modulated signal to be demodulated. However in this case a partially coherent detection is used here where a one-bit delay is use. Figure 80 and Figure 81 illustrate the concept of the partially coherent detection scheme that was applied in this MATLAB SIMULINK model.

54
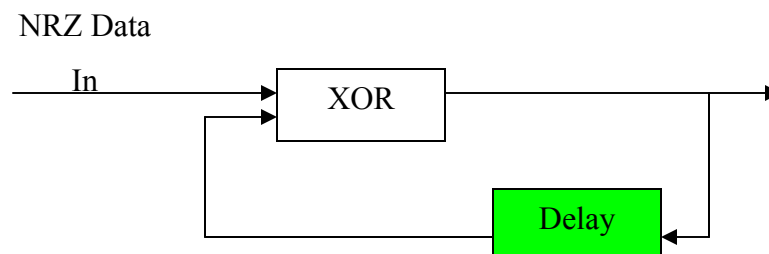
Figure 80: Block diagram of the differential coding system at the transmitter

From the block diagram in Figure 80, the NRZ data will be produced by the Bernoulli Binary Generator. This data is then delayed by one bit and then an XOR logical operation will be performed to produce the DPSK electrical data.

At the receiver, the DPSK electrical is also delayed by one bit after which an XOR logical operation is performed to achieve the decoded NRZ output Figure 81.
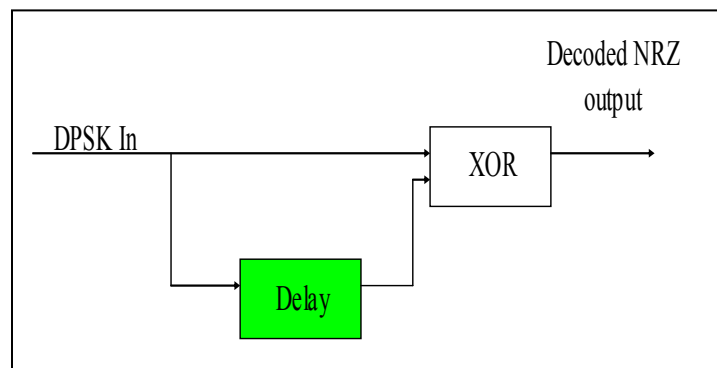
(a)

Optical balanced receiver - DPSK
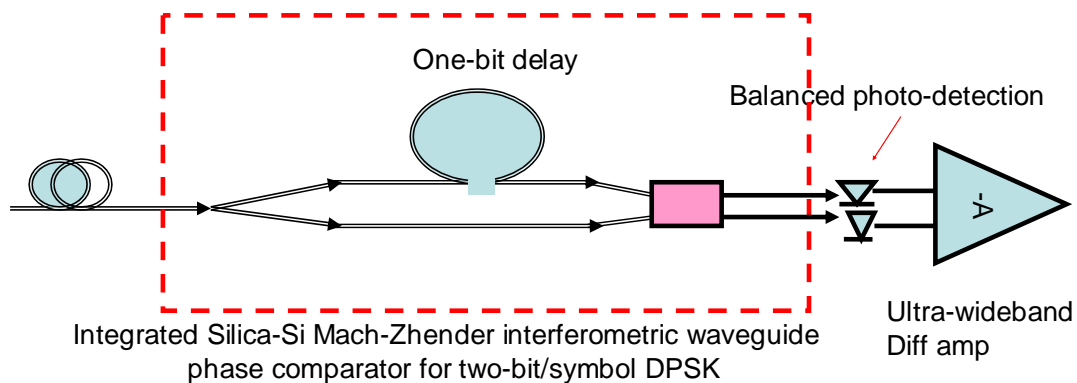
(b)

The DPSK electrical signal is then used to drive an MZIM to produce a DPSK optical signal. As the XOR logical operation is used, a '0' bit will represent no change in bits and a '1' bit will represent a change in bits. Hence at the DPSK transmitter, for each '1' bit which represents a change in bit, the optical phase will be introduced with a π phase change and a '0' bit will be left unchanged.
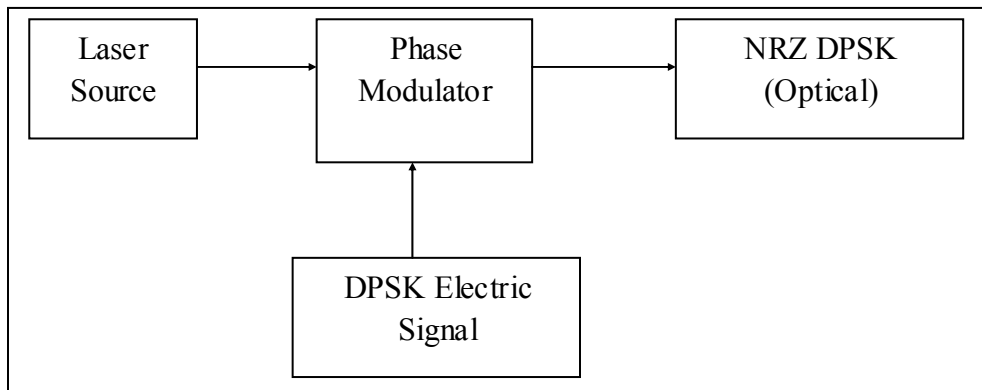
Figure 82: Block diagram of the NRZ-DPSK transmitter
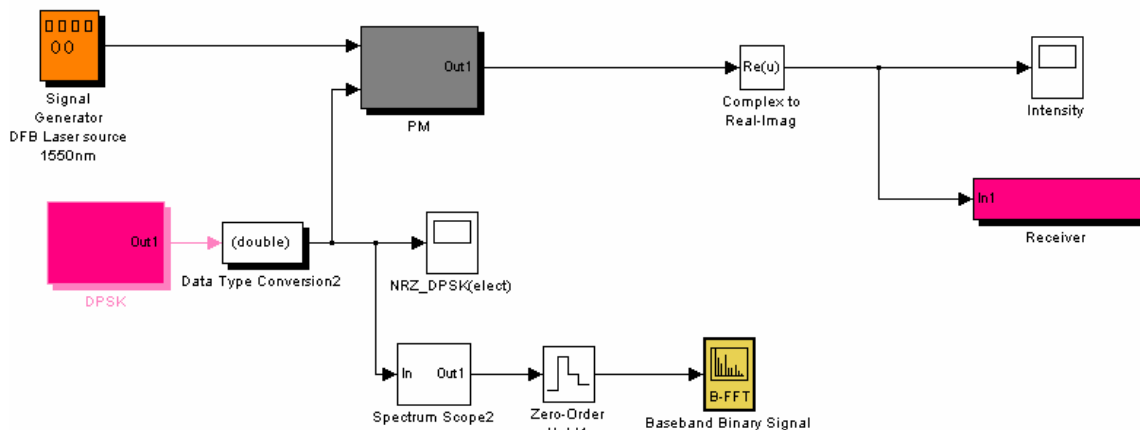
4.7.1 DPSK block
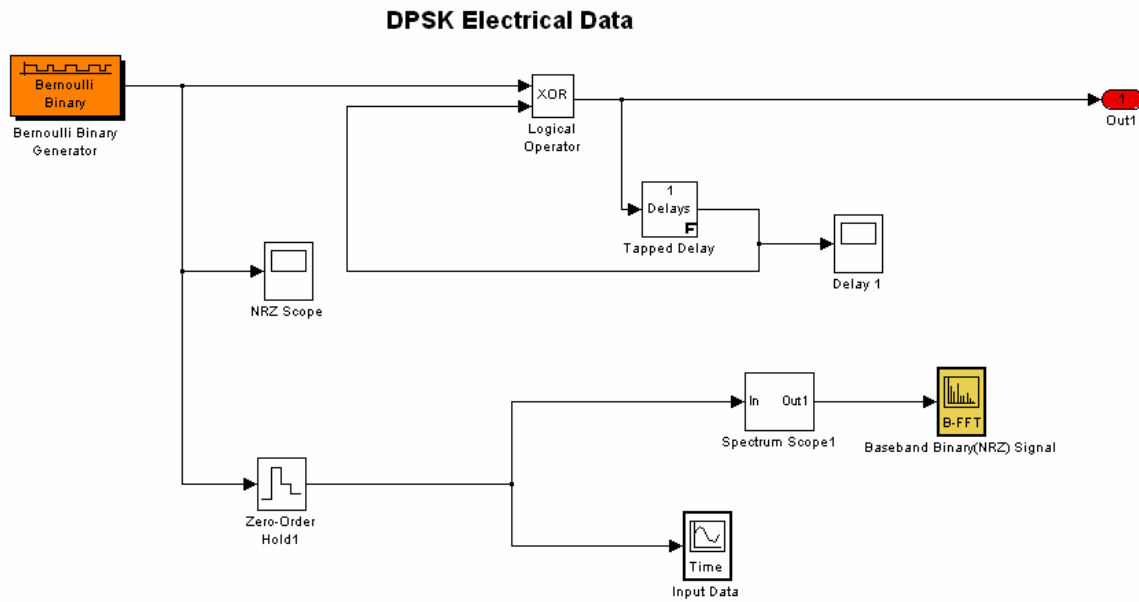
Figure 84: DPSK electrical data

As explained above, the DPSK electrical data is produced using the partially coherent detection scheme.

4.7.2 PM block

57
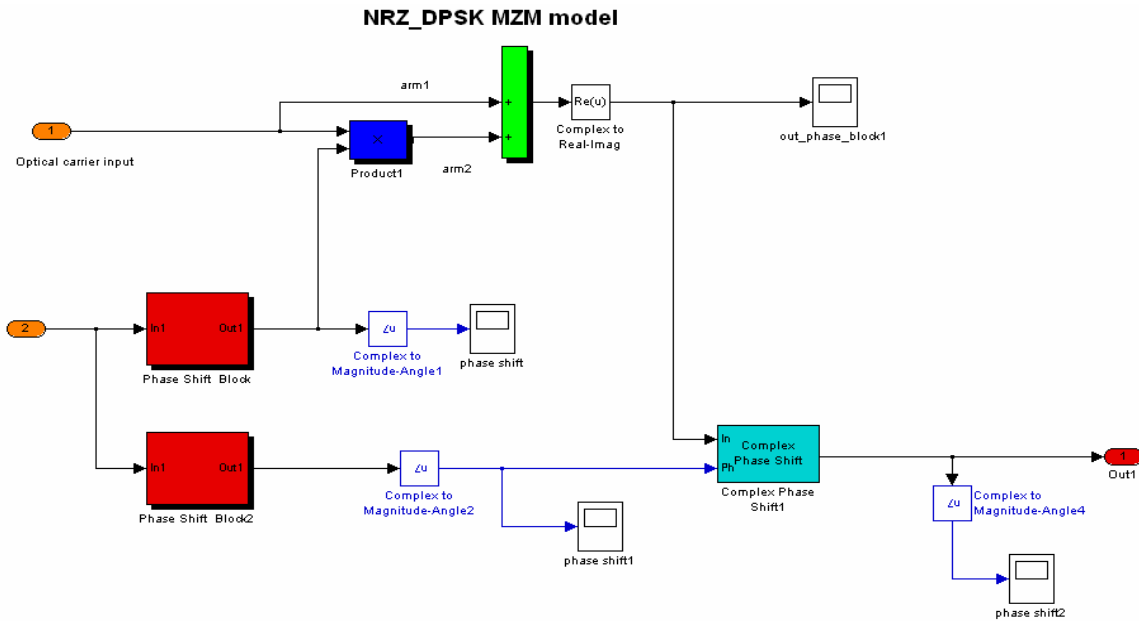
Inside the PM block, the input port 1 as seen in Figure 85 is the optical carrier and input port 2 is the DPSK electrical data. To produce the NRZ-DPSK optical signal, the electro optic intensity modulator (MZIM) was used again. The complex phase shift block is then used to phase shift the optical phase by π when a '1' bit is detected and a phase shift of zero when a '0' bit is detected.

Receiver block
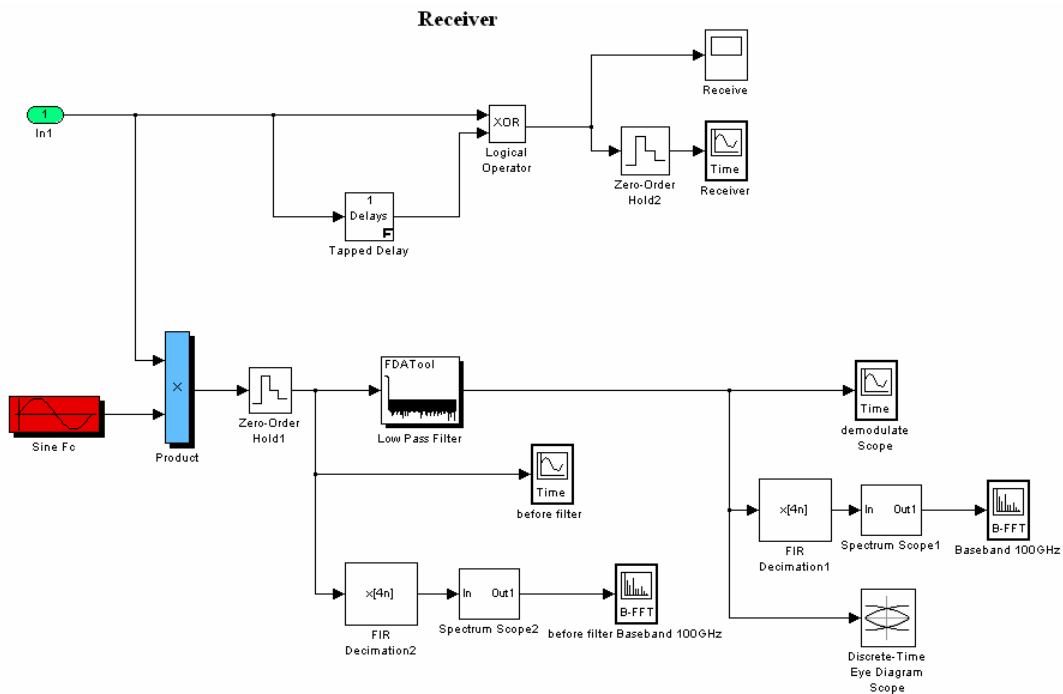
Figure 86: Simulink model inside the receiver block employing a single PD.

Inside the receiver block, the NRZ-DPSK optical signal is then demodulated and passed through a low pass filter to remove the carrier.

58
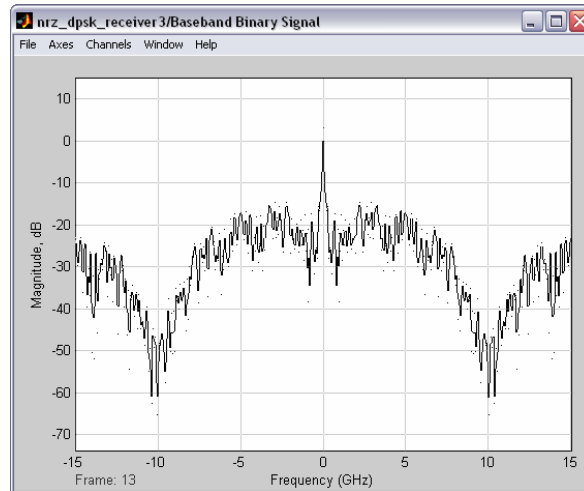
Figure 87: Spectrum scope observed at the baseband NRZ DPSK

Figure 87 illustrates the spectrum scope observed at baseband, the spectrum scope observed without presence of a carrier component.
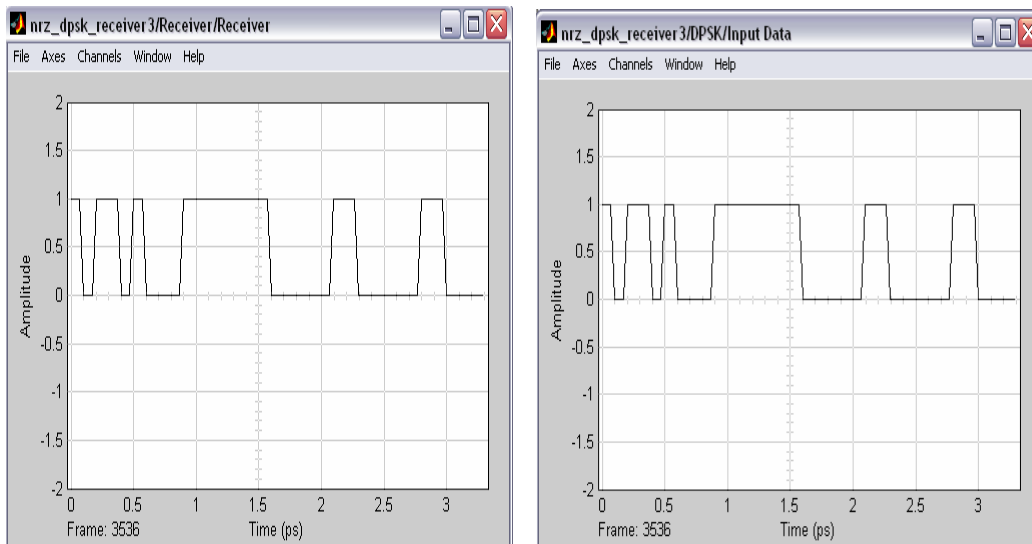
Figure 88: Scope displaying (a) input data from the Bernoulli Binary Generator (b) data received at the receiver.
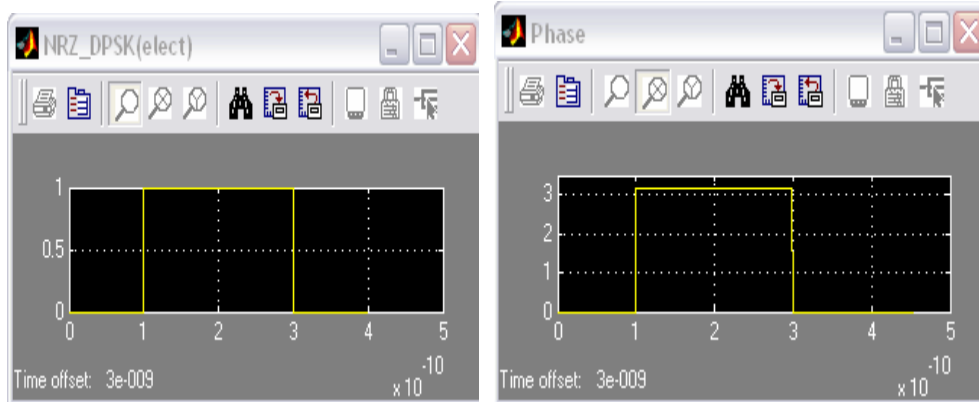
Figure 89: Scope displaying (a) the NRZ-DPSK electrical data.(b) the DPSK transmitted phase.

Observing the scopes in Figure 89, it can be seen that a DPSK electrical data of a '1' bit will result in a π phase shift in the optical phase. And a '0' bit will result in no phase shift in the optical phase.
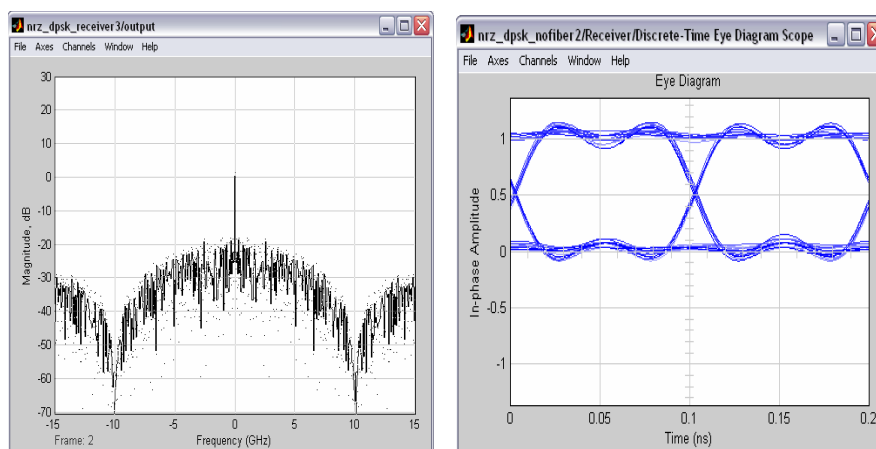
Figure 90: (a) Spectrum scope observed at the receiver (b) Eye diagram in electrical domain observed at 10 Gb/s at the receiver end, BER = 10e-12

4.8. *RZ Differential Phase Shift Keying (DPSK) Model*

Figure 91 shows the block diagram of the RZ-DPSK transmitter design in MATLAB SIMULINK where an additional intensity modulator was added. With this additional MZIM, the NRZ-DPSK optical signal from output of the PM block will be sampled by a pulse generator to achieve the desired RZ-DPSK signal.
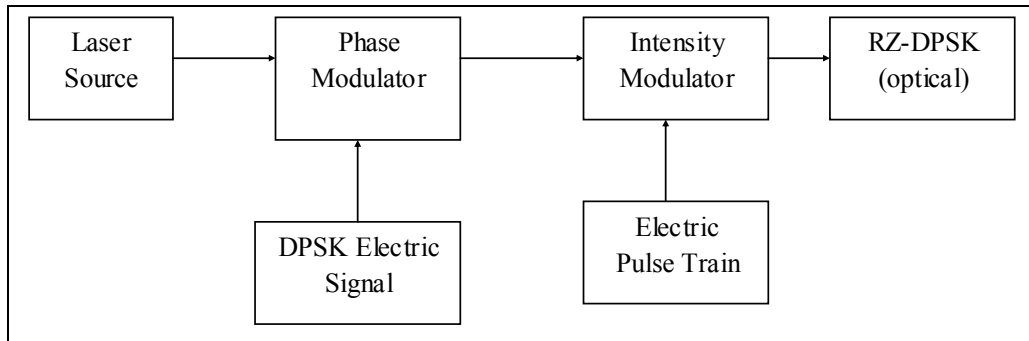
Figure 91: Block diagram of the RZ-DPSK transmitter
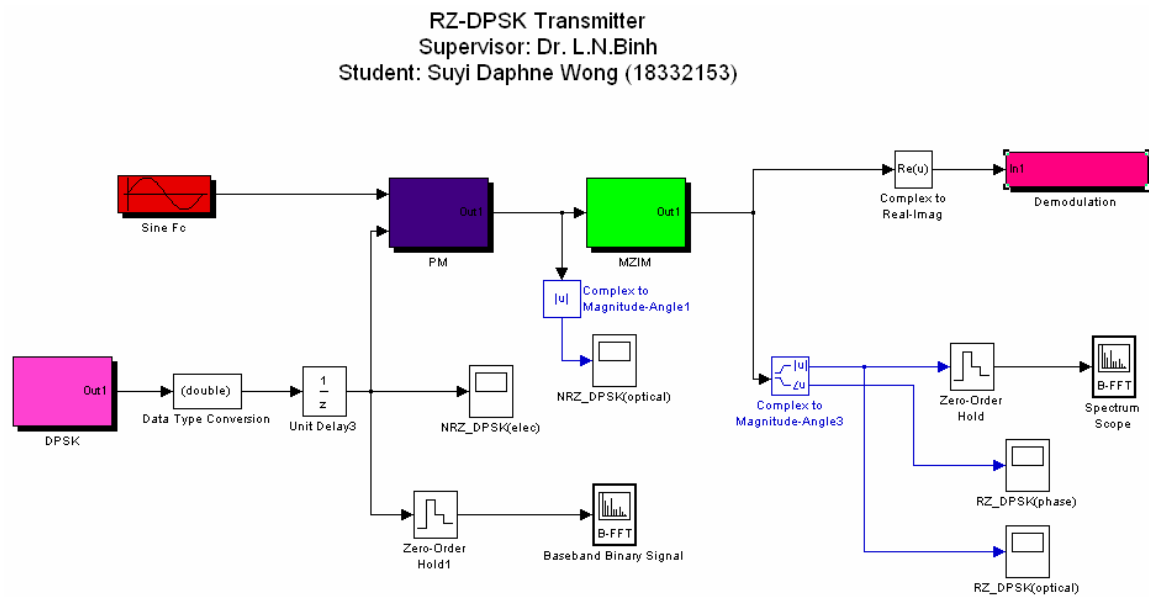
Figure 92: RZ-DPSK MATLAB SIMULINK model

| (a) | (b) | (c) |

61
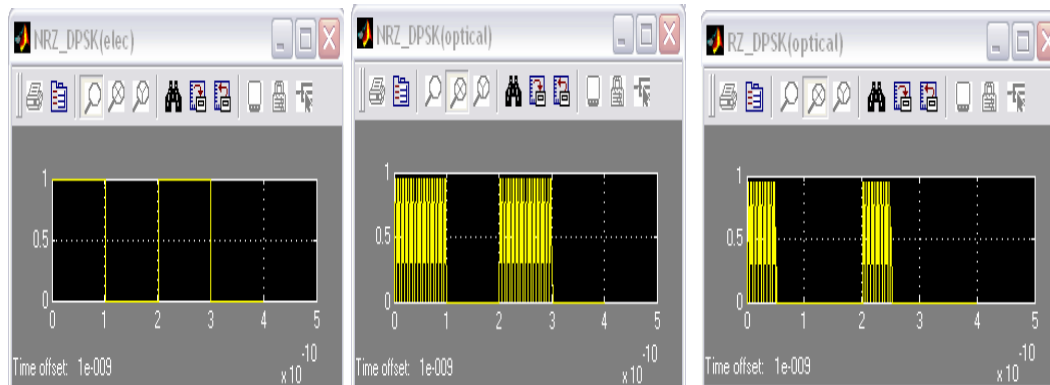
Figure 93: Scope displaying (a) NRZ-DPSK electrical data signals (b)the optical NRZ-DPSK signal (c) the RZ-DPSK signal

Figure 93 illustrates the RZ data from the output of the intensity modulator. *Figure 94* illustrates the 　phase shift observed when a '1' bit is received and a 0 phase shift when a '0' bit is received. The eye diagram is illustrated in *Figure 95*.

(a)   (b)
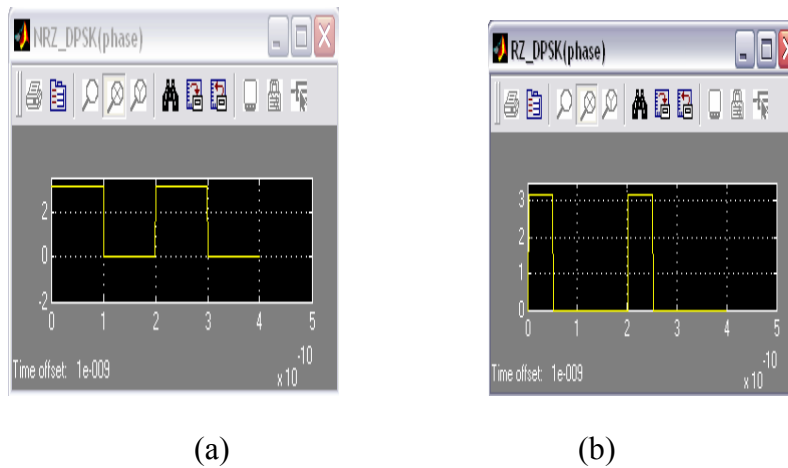
Figure 94: Scope displaying (a) the NRZ-DPSK transmitted phase (b) the RZ-DPSK transmitted phase
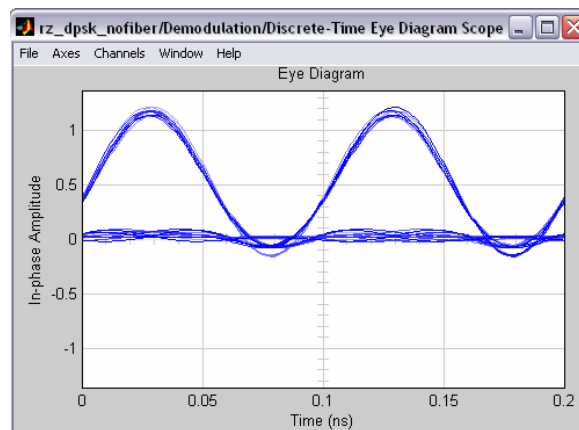
Figure 95: Eye diagram observed of 10 Gb/s RZ-DPSK using single PD detection.

5.   CONCLUDING REMARKS and CHALLENGES

When implementing the MATLAB SIMULINK models for the various modulation formats, the accuracy of the model is a very important factor. Many difficulties were faced when implementing the MZIM in MATLAB SIMULINK, mainly:

62

- The implementation of the voltage bias of the MZIM in MATLAB SIMULINK.

- The non-linearity of the MZIM and thence the patterning effects, hence system power penalty

- The implementation of driving voltage (V_π) and its effect on the voltage bias.

- Optical fiber losses at the input and at the output of the MZIM.

- Signal to Noise (SNR) generation within the MZIM.

- The modeling of the non-linearity chirping of the MZIM.

- Correct sampling of the formats when outputting the eye diagrams for the required results.

The difficulties have been resolved to produce an accurate MATLAB SIMULINK model for various modulation formats. They are:

- To measure the bit error rate of the MZIM, some of the measuring equipment has to be left for a long period of time until the result stabilizes.

- The actual polarization of the input optical strength.

- The eye diagrams produced had unwanted noise from the optical fiber and from the system itself. This had made readings difficult to be analyzed.

- The photo-detector required to convert optical signal to electrical signal can only operation between -5 dBm to 5 dBm. Therefore, we had to be very careful with the experiment settings to ensure that we do not damage any equipment. Limiting our MATLAB simulations to be within these values also.

- The input of the bit pattern generator has to be synchronized with the signal Analyzer to produce the eye-diagram.

Due to the complexity of the SIMULINK models, some of the software problems have delayed the outcome of the work. There are some parameters that can be easily implemented by hardware; however it proved to be more difficult to model it in

software. An accurate model in SIMULINK is needed for comparisons with the experimental results.

Improvements can be made on the current design in SIMULINK as a few assumptions are made In the process of designing this SIMULINK model. One of the assumptions made was that the voltage bias quiescent point was zero; this will set the voltage bias point of the model to be zero volts. From the experimental results that were achieved in Singapore, the quiescent point was around 4V which was between the maximum point of 2.4V and the minimum point of 6.5V.

Another improvement that can be made on this MATLAB SIMULINK model is to model this system with an EDFA model based on practical EDFAs. The photo detector only operates between -5dBm and 5dBm. However in this MATLAB SIMULINK design model, only the noise from the Gaussian noise generation block (AWGN) was taken into account. The ASE noise contributed by the EDFA has not been taken into account in this part but fully superimposed on signals in the next part of the series. The principal objective of this part is to demonstrate the Simulink model for modulation format DPSK..

As there are always constant changes and improvements in optical communication systems, especially on modulation techniques, this SIMULINK model allow users to simulate and modify various modulation formats to suit long-haul high speed DWDM transmission system for system design and planning.

The design of this SIMULINK model can be compared with the practical results achieved. The experimental results serve as a very good guide to compare our simulated results to ensure the validity of the model. Comparing the BER results from the SIMULINK MATLAB model and the BER from the experimented results, it can be concluded that the results achieved in MATLAB are accurate.

6. REFERENCES

[1]   S. V. Kartalopoulos, *"Introduction to DWDM technology: Data in a rainbow"*: J Wiley, 2001.

[2]   L. N. Binh, *ECE 4405 Lecture Notes on Optical Communications Systems*. Melbourne, Australia: MiTec, 2003.

[3]   J. Hecht, *Understanding Fiber Optics*: Prentice Hall, 1997.

[4]   J. Armstrong, ""Simulink Optical Simulator"," in *Electrical and Computer Systems Engineering*. Clayton, Australia: Monash, 2003, pp. 62.

[5]   G. P. Agrawal *Fiber-optic Communication Systems*, 2nd ed. N.Y.: Academic Press, 2002.

[6]   V. Sauvé, ""DPSK offers alternative high-speed signal modulation",." *WDM Solution*, vol. PennWell, 2002.

[7]   R. Hui, Zhang, S., Zhu, B., Huang, R.C., Allen, D., " "Advanced Optical Modulation Formats and Their Comparison in Fiber-Optic Systems", Technical report," 2004.